Progress in Oceanography 217 (2023) 103106

Contents lists available at ScienceDirect

Progress in Oceanography

journal homepage: www.elsevier.com/locate/pocean

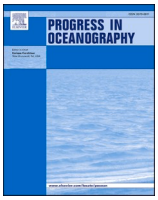

New insights into the Barents Sea *Calanus glacialis* population dynamics and distribution

Johanna M. Aarflot [a,*], Elena Eriksen [a], Irina P. Prokopchuk [b], Camilla Svensen [c], Janne E. Søreide [d], Anette Wold [e], Morten D. Skogen [a]

[a] Ecosystem Processes Group, Institute of Marine Research (IMR), Bergen, Norway
[b] Polar Branch of FSBSI "VNIRO" ("PINRO" named after N.M. Knipovich), Murmansk, Russia
[c] Department of Arctic and Marine Biology, UiT The Arctic University of Norway, Tromsø, Norway
[d] The University Centre in Svalbard (UNIS), Tromsø, Norway
[e] Norwegian Polar Institute, Tromsø, Norway

ARTICLE INFO

Keywords:
Individual-based model
ODD protocol
NORWECOM.E2E
Reproduction
Seasonal dynamics
Transportation

ABSTRACT

Arctic copepods are major grazers and vital food for planktivores in polar ecosystems but challenging to observe due to remoteness and seasonal sea ice coverage. Models offer higher spatio-temporal resolution, and individual-based models (IBMs) are useful since they incorporate individual variability which characterizes most copepod populations. Here, we present an IBM of the Arctic copepod *Calanus glacialis*, a key secondary producer in polar regions of the Barents Sea. The model is coupled to a three-dimensional physical-biological model, and an IBM for the Atlantic congener *C. finmarchicus*. We use the model to fill seasonal "gaps" between discontinuous spatio-temporal sampling for studying the spatial and seasonal population dynamics. Our simulations suggest that, across the Atlantic and Arctic domains of this ecosystem, total population egg production peaks in July, and copepodid 3 is the main overwintering stage descending to deeper overwintering depths between July and September. Total population biomass peaks at 5 times higher carbon mass than the seasonal minimums and is driven by the seasonal build-up of biomass in stages C4, C5 and adults. Ocean currents spreads the population over a large area, though with a clear spatial separation between *C. glacialis* and *C. finmarchicus* in the northern and southern Barents Sea, respectively. There is a mixture between 1- and 2-years life cycles in the model population, and those who require two diapause phases to reach maturity have spent a larger part of their life north of 77°N, where temperatures are colder and the growth season shorter than further south. A remaining question is where the source population of *C. glacialis* in this ecosystem resides, and whether the population relies on local survival and reproduction or continuous supply from a source population outside the Barents Sea.

1. Introduction

Copepods are key grazers in polar ecosystems, and their numerous presences combined with high individual lipid contents makes them vital food for fish, whales and seabirds (Bouchard and Fortier, 2020; Karnovsky et al., 2003; Kattner and Hagen, 2009). Arctic copepods have been less studied than boreal species since investigating high-Arctic remote populations is associated with high costs and temporal inaccessibility due to sea ice. Models have higher temporal and spatial resolution than *in situ* observations and can be useful both for *knowledge validation* (Aarflot et al., 2022) and to fill gaps or shed light on unresolved questions regarding a species in its environment. Here, we present an individual-based model (IBM) of the Arctic copepod *Calanus glacialis* in the Barents Sea ecosystem.

The Barents Sea is a sub-Arctic shelf sea bordering the Arctic Ocean in the north and the Norwegian and Russian coasts in the south. It is often described as a flow-through shelf system (Carmack et al., 2006) and dominated by water masses of both Atlantic and Arctic origin (Fig. 1). Arctic waters enter the Barents Sea in the northeast and north and provide cold arctic conditions in northern regions with sea ice coverage for several months each year. Maximum and minimum ice extent is generally found in March and September, respectively (Onarheim et al., 2018). In these regions, *C. glacialis* is considered a key grazer and secondary producer while the more temperate congener

* Corresponding author.
E-mail address: johanna.aarflot@hi.no (J.M. Aarflot).

https://doi.org/10.1016/j.pocean.2023.103106

Available online 18 August 2023

C. finmarchicus dominates in Atlantic water masses advected from the Norwegian Sea in the southwest (Aarflot et al., 2018) (Fig. 1). The northern Barents Sea has been characterized as a "hot spot" for summer feeders such as pelagic and younger stages of demersal fish species, seabirds and marine mammals (e.g. Eriksen et al., 2017; Falk-Petersen et al., 2000b; ICES, 2018), and may become an even more important foraging arena with future declines in sea-ice (Langbehn et al., 2023). Hence, *Calanus* spp. are important for the energy transfer not only between different tropic levels in this region, but also between different geographical areas within and outside of the Barents Sea where predators will return after the heavy feeding season (ICES, 2021; Langbehn et al., 2023). Arctic regions of the Barents Sea have been characterized as locations under extensive pressure from climate change (Comiso and Hall, 2014; Lind et al., 2018), and with continuous warming the Barents Sea arctic ecosystem is expected to make a transition towards "Atlantic" conditions (Ingvaldsen et al., 2021).

Such Atlantification of the Barents Sea is often assumed to increase the dominance of *C. finmarchicus* over the Arctic sibling *C. glacialis* (e.g. Hirche and Kosobokova, 2007), with negative consequences for size-selective planktivorous fish and sea birds (Vogedes et al., 2014). The expectation that *C. glacialis* will struggle in a Barents Sea transitioned towards Atlantic conditions implicitly assumes that *C. glacialis* will not thrive in a warmer, ice-free environment. Yet, this species also sustains local populations in deep fjords in Norway which experiences up to 10–15 °C in surface layers in summer (Niehoff and Hirche, 2005; Choquet et al., 2017).

Population-wide responses of copepods to climate change cannot be predicted from changes in environmental conditions directly because the response will also depend on a species' behavioral and life history traits (Banas et al., 2016). Like most copepod species, *C. glacialis* is characterized by a high degree of individual variability in development and life history, presumably resulting from local adaptations to environmental conditions. In the Barents Sea, *C. glacialis* has been suggested to have a life cycle of 1–2 years (Melle and Skjoldal, 1998), and overwintering copepodids range from C3 to adult females (Daase et al., 2013). Observations of active individuals in surface waters during winter have, nonetheless, raised questions regarding plasticity in overwintering strategies and the potential for skipping diapause (Freese

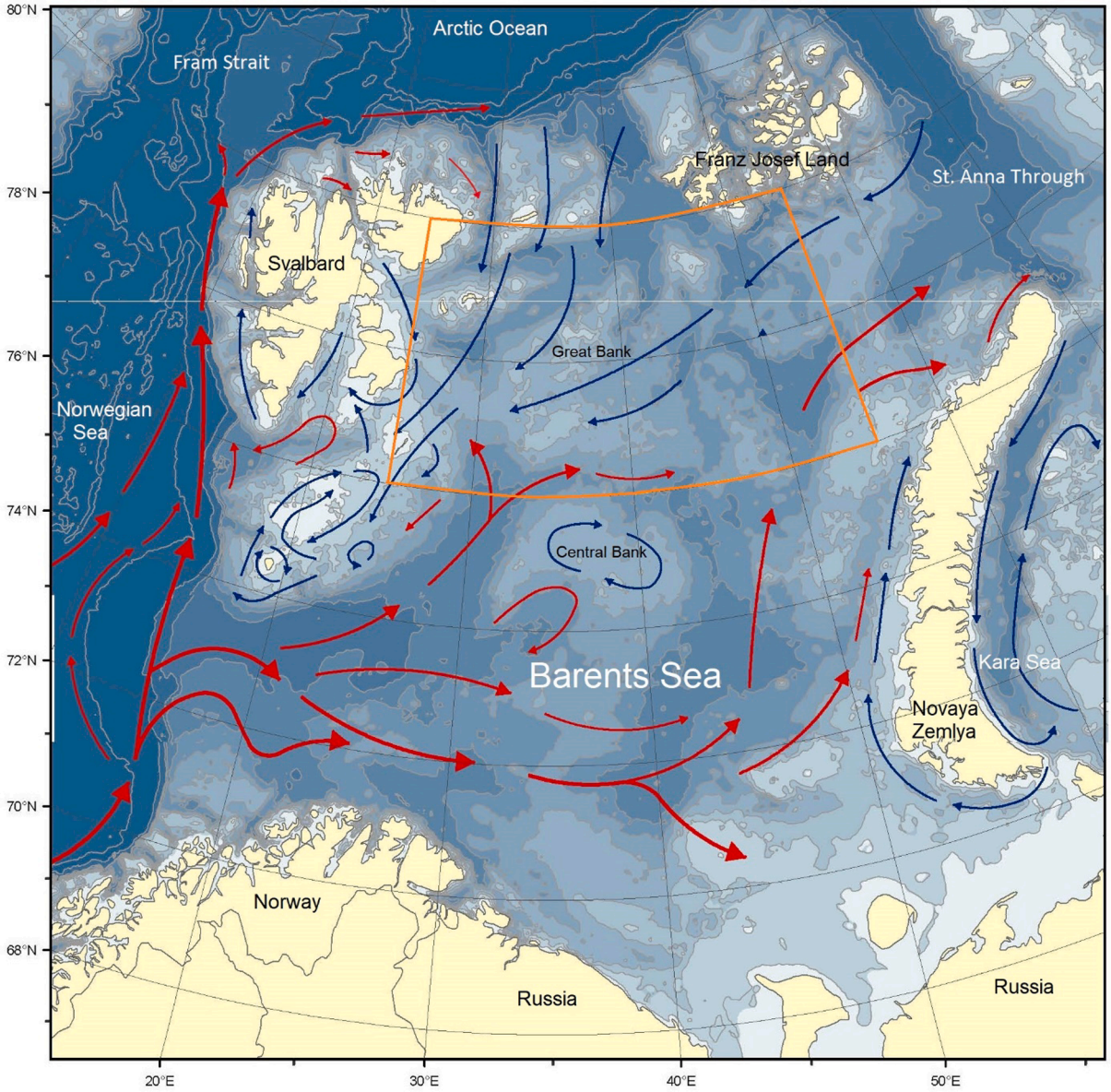

Fig. 1. Barents Sea study region with major surface currents in red (Atlantic water) and blue (Arctic water). Yellow lines frame the area of release for the initial *Calanus glacialis* model population.

et al., 2016; Hobbs et al., 2020). Phytoplankton is the primary food source for *C. glacialis* in spring (Juul-Pedersen et al., 2006) but it is also considered an omnivore forager where microzooplankton is included in the diet (Campbell et al., 2009), the latter presumably more important in the post-bloom phase (Svensen et al., 2019). In addition, ice-algae are an important nutritious food early in the season which prolong the growth season for *C. glacialis* in seasonally ice-covered regions (Runge and Ingram, 1991; Søreide et al., 2010). Egg production in *C. glacialis* has been suggested to be both food dependent and food independent (income *versus* capital breeding; Varpe et al., 2009), and to rely on ice-algae for early maturation and egg production in regions with seasonal ice-cover (Søreide et al., 2010; Daase et al., 2013).

IBMs are useful for simulating dynamics of natural populations with high individual variation in for instance behavior, fitness and genotypes (DeAngelis and Grimm, 2014). The name of the model reveals its advantage; the approach of using individuals rather than populations as a basic unit, whereby the population properties emerge from the sum of individual properties. Coupling IBMs to three-dimensional hydrodynamic models enables the study of population-level properties resulting from environmental variation. Our IBM of *C. glacialis* is coupled to a three-dimensional ecosystem model (NORWECOM.E2E; Aksnes et al., 1995; Skogen et al., 1995) encompassing physics, a nutrients-phytoplankton-zooplankton-detritus (NPZD) model and an IBM of the Atlantic congener *C. finmarchicus* (Hjøllo et al., 2012; Huse et al., 2018). The IBM presented here is parametrized based on existing knowledge of *C. glacialis* from the Barents Sea and adjacent regions encompassing individual variation in growth and phenology.

Here, we use the model to study the spatial distribution and seasonal population dynamics emerging from an overwintering population released in the northern Barents Sea (Fig. 1). Environmental variation in the model domain will lead to individual variation in growth and development, whereby the seasonal population dynamics are an emergent property of the model. We use the model to 1) evaluate the magnitude, timing and driving forces of seasonal biomass fluctuations, 2) investigate whether individual variation in growth and development can be attributed to environmental variation, and 3) identify mechanisms structuring the spatial distribution of *C. glacialis* in the Barents Sea. We also use our results to discuss how a changing climate may act on future *Calanus* distributions in this ecosystem.

2. Materials and methods

2.1. 3D environment: NORWECOM.E2E

NORWECOM.E2E (NORWegian ECOlogical Model system End-To-End) brings together a NPZD model for plankton and nutrient cycling (Aksnes et al., 1995; Skogen et al., 1995, 2007) and several IBMs developed for zooplankton and fish (Hjøllo et al., 2012, 2021; Utne et al., 2012; Huse et al., 2018; Hansen et al., 2021; Aarflot et al., 2022). Modules in NORWECOM.E2E are two-way coupled so that growth of prey species provides food densities for modules one trophic level above, and feeding is implemented as mortality at the trophic level below. In the present study, we utilize the NPZD and an IBM for *C. finmarchicus* in addition to a new IBM developed for *C. glacialis* (described below).

The NPZD is coupled to physical forcing from an ocean circulation model (ROMS; Shchepetkin and McWilliams, 2005) with a horizontal resolution of approximately 4x4 km (Lien et al., 2013). From this, the NPZD receives hourly input on light, hydrography, and the horizontal and vertical movement of water masses. Prognostic variables are dissolved inorganic nitrogen, phosphorous and silicate, two types of phytoplankton (diatoms and flagellates), two detritus pools (nitrogen and phosphorus), diatom skeletal (silica) and oxygen. Two sizes of generic grazers (micro- and mesozooplankton) are included in the NPZD, and processes include primary and secondary production, grazing, respiration, algae death, remineralization of nutrients in water column and sediments, self-shading, turbidity, sedimentation, resuspension, sedimental burial and denitrification. Parametrizations of biochemical processes are taken from the literature (see Aarflot et al., 2022 and references therein).

2.2. New Calanus glacialis individual-based model

Our IBM description follows the overview, design concepts and details (ODD) protocol for describing IBMs developed and updated by Grimm et al. (2020, 2010,2006), which entails outlining the model purpose, structure, and processes before elaborating detail on submodels and equations. Numerical copepods are hereafter referred to as "compupods" following Maps et al. (2014), for easier separation between model entities and actual organisms.

2.2.1. Purpose

The IBM for *C. glacialis* builds on the existing *C. finmarchicus* IBM in NORWECOM.E2E but has been modified to capture key traits of *C. glacialis* in the Barents Sea ecosystem. Our aim with this IBM is to advance our understanding of the life history, seasonal dynamics, and spatial distribution of a major grazer in the northern Barents Sea.

2.2.2. State variables and scales

Model entities are individual compupods that develop from eggs through six nauplii (N1-N6) and five copepodid stages (C1-C5) before reaching the adult stage (C6). Individuals are modelled in a three-dimensional environment which sets the ambient temperature, light, food availability and horizontal advection. The state of an individual at each time step is defined by 13 attributes ('attribute vector', Huse et al., 2018) including the developmental stage, structural weight, lipid reserves and horizontal and vertical position (Table 1). Compupods are associated with four behavioral and life history traits ('strategy vector', Huse et al., 2018) which are inherited from parents to offspring and remain fixed over the life cycle (Table 2). These include the overwintering depth (OWD), day of year for waking up from overwintering (wake-up-day; WUD), day of year after which descent to overwintering may occur (enter-diapause-day; EDD) and the allocation to soma ratio (ASR) which sets the ratio of ingested food allocated into somatic growth (remains are stored as lipids).

To overcome computational constraints when modelling high population abundance, we adopt the superindividual (SI) approach (Scheffer et al., 1995) where one model individual represents a cohort of identical siblings (see Section 2.2.5).

2.2.3. Process overview and scheduling

Processes controlling the compupods are growth, movement, mortality, and reproduction. Growth, movement, and mortality are

Table 1
Attributes of superindividuals characterizing individual states at each time step of the simulations.

Attribute	Description
mynumb	Unique identifier for each superindividual
alive	0 = dead, 1 = alive
inumb	Number of identical siblings represented by superindividual
stage	Egg, Nauplii N1-N6, Copepodid C1-C6
age	Age in days
lstage	Stage longevity in days
sweight	Structural weight in µg C
lipids	Lipid reserves in µg C (CIII – adults)
moult	Moult cycle fraction (eggs and N1-N2)
maxegg	Number of eggs to be spawned
cumeggs	Accumulated number of eggs spawned
position	Grid position (x, y, z)
activity level	0 = diapause, 1 = active, 2 = descending, 3 = ascending
parent	Identity of parent superindividual
sex	0 = male, 1 = female
death	Cause of death

Table 2
Strategy of superindividuals inherited from "parent" and remaining fixed over the lifecycle.

Strategy	Description	Values at initialization	References
Wake up day (WUD)	Day of year for ascent from overwintering	Normal distribution with mean 70 and SD 30 (early March +/−30 days)	Daase et al. (2013)Bandara et al. (2016)
Enter diapause day (EDD)	Day after which descent to overwintering may occur if/when enough lipid reserves	Random day between 196 and 256 (mid-July to mid-September)	Daase et al. (2013)Bandara et al. (2016)
Overwintering depth (OWD)	Vertical position for overwintering individuals	Random depth between 200 and 500 m	Bagøien et al. (2001)Falk-Petersen et al. (2009)Bandara et al. (2016)
Allocation to soma ratio (ASR)	Fraction of assimilated food allocated to somatic growth; remains are invested in lipid reserves	Fixed at 0.5 in current simulations	Lee et al. (2006)

simulated by hourly timesteps, while reproduction is simulated once every 24 h.

Based on Daase et al. (2011) we set nauplii stage N3 as the first feeding stage, and development up to this point is temperature-dependent following a Belehradek's function and estimates for *C. glacialis* eggs and nauplii from Jung-Madsen and Nielsen (2015). From N3, growth is estimated as a function of temperature, food density and compupod size using a functional response type 2 model (Carlotti and Wolf, 1998) and field estimates for *C. glacialis* daily ingestion rates (Campbell et al., 2016). Compupods feed on phyto- and microzooplankton from the NPZD, in addition to an ice-algae food source in spring/summer months with the availability determined by light and sea ice extent. Growth is invested in full into the structural weight (N3–C2) or divided between structural weight and lipids (C3–C6). Compupods will change stage when their total weight (*sweight* + *lipids*) reaches a stage-specific molting weight (Table 4).

Movement is both vertical, on diel and seasonal rhythms, and horizontal simulating passive drift with ocean currents. We assume equal probabilities of becoming females and males at stage C6, and only female compupods give rise to new offspring. Females spawn in batches (Hirche and Bohrer, 1987; Pasternak et al., 2002) until the total lipid reserves are drained or a maximum number of eggs is reached (Table 4). Male C6 compupods are taken out immediately after molting, so the sex-ratio in the model environment will be skewed towards dominance of females (Daase et al., 2018). Other mortalities comprise stage-specific natural mortality, starvation, visual and tactile predation, spawning exhaustion and a geographically bound additional mortality rate. The total rate is adjusted based on population size simulating density-dependence and as a means of tuning the model to better fit with empirical observations.

2.2.4. Design concepts

Emergence and adaptation. Individual traits like size emerge from the interactions between compupods and their environment, and spatial and temporal population dynamics emerge from the sum of individual traits. Life strategies (Table 2), on the other hand, are inherited from the parent and remain fixed over a compupod life cycle. As the population develops, the "gene" frequency (life strategies) at population level will to some degree be subject to adaptation due to varying reproductive success among superindividuals. This may increase the overall fitness of the population over time.

Sensing and interaction. Compupods are assumed to be aware of their inherited strategies (wake-up day, enter diapause day and overwintering depth; Table 2) and can sense the state of own lipid reserves and vertical position in addition to the day number, for deciding when to descend to and ascend from overwintering. Compupods may also separate between day and night and sense the depth of the chlorophyll maximum, used for setting the vertical position in diel vertical migrations. Grazing by compupods affects phyto- and microzooplankton in the NPZD, and food sources from the NPZD are shared between the *C. glacialis* and *C. finmarchicus* IBMs (see Section 2.1). Feeding is modelled one individual at a time and food sources are greatest for those who feed first. Hence there is competition for food both between compupods from the same IBM and between the *C. glacialis* and *C. finmarchicus* IBMs.

Stochasticity. Genes for the wake-up and enter diapause days and the overwintering depth are initiated at random within a fixed range taken from the scientific literature (Table 2). Feeding order is computed at random each time step, both regarding which of the *C. glacialis* and *C. finmarchicus* IBM that feeds first, and between compupods from the same IBM. There is also a random walk component in the horizontal movement of a superindividual to represent sub-grid diffusion processes, and the vertical position for eggs-N2 is set at random within the top 40 m. Sex is chosen at random in a 1:1 probability ratio when a superindividual reaches the adult stage.

Collectives. Each superindividual represents one or more identical compupods which are spawned at the same time and have identical attributes and strategies throughout the simulations, but that die off one by one.

Observation. IBM data on superindividuals and their attributes are stored every 48 h and can be analyzed on a detailed level. We evaluate both individual growth and movement of compupods from different areas, in addition to population level development and spatial distribution. Fluxes between different species and processes in NORWECOM. E2E are stored and analyzed by daily time steps.

2.2.5. Initialization

The model was initiated with an overwintering population of 1.5 million tonnes (MT) carbon, based on Tande (1991) who estimated a *C. glacialis* standing stock of 3 g dry weight (1.8 g carbon) m^{-2} in the Barents Sea, and assuming that the distribution of *C. glacialis* covers half of the 1.6 million km^2 Barents Sea area (Carmack et al., 2006). For comparison, 1.5 MT is about half the population size assumed for the congener *C. hyperboreus* overwintering population in the Greenland Sea (Aarflot et al., 2022; Visser et al., 2017).

To create an initial population field for our main simulations, the initial biomass was distributed into 40 000 superindividuals released uniformly in the northern Barents Sea between 25 and 55°E and 76–80°N (see Fig. 1 and overview of simulations in Table 3). The superindividuals comprised equal amounts of C4 and C5 compupods, since these are considered the dominant overwintering stages here (Daase et al., 2013), and were given weights of 55 and 390 μg C, respectively (50 % as lipid reserves, Table 2). Simulated "genes" for the seasonal vertical migrations (wake-up and enter diapause days, overwintering depth) were initiated within ranges taken from observational studies (Table 2). Following, the model was run for 10 years with (hourly) physical forcing from year 2000, which is the first year with available forcing on 4 km resolution. The model field on January 1 after the 10th run (10 × year 2000) was saved and used as the initial population field for the current study.

In our main simulation, we have chosen to use physical forcing from

Table 3
Overview of simulations and forcing employed, outputs from the basic simulation (simulation 3) are analyzed in the current study.

Simulation	Purpose	Description	Forcing (reason)
1	Establish initial population field	40 000 superindividuals released uniformly in the northern Barents Sea between 25 and 55°E and 76–80°N. Equal amounts of C4 and C5 compupods. Dynamics allowed to evolve over 10 runs (1 run = 1 year).	Year 2000 (first year available), hourly time-step, 4 km spatial resolution.
2	Spin-up for basic simulation	Starting with final population field from simulation 1, dynamics evolving over 25 runs.	Year 2013 (data-availability), hourly time-step, 4 km resolution.
3	Basic simulation	Starting with end population from simulation 2, dynamics evolving over 25 runs.	Year 2013 (data-availability), hourly time-step, 4 km resolution.

2013 because this is a year where we have *C. glacialis* abundance by stage data from northern regions of the Barents Sea to which we can compare our results (see Discussion). We use physical forcing from only one year to have control over the environmental conditions when evaluating model performance. Our main simulation starts on January 1, 2013, and the biology is allowed to evolve over 50 years with physics from 2013, where the first 25 are used as "spin-up" years while the latter half is our "basic simulation" years. Results presented in this paper are from the basic simulation only.

2.2.6. Input data

Physical forcings are taken from a simulation with the Regional Ocean Model System (ROMS) (Shchepetkin and McWilliams, 2005) providing hourly values for temperature, salinity, light, currents, wind and sea ice on 4x4 km horizontal resolution and for 20 depth layers. The output of the ROMS model has been used to produce the Nordic Seas 4 km numerical ocean model hindcast archive (SVIM) (Lien et al., 2013) for the period 1960–2019 (available online; Norwegian Meteorological Institute, Institute Of Marine Research, 2015). The IBM also receives biological input (phytoplankton and microzooplankton abundance) from the NPZD in NORWECOM.E2E on the same temporal and spatial scale as the physical input.

2.2.7. Submodels

Movement. The IBM simulates both diel and seasonal vertical migration by which compupods change the depth position (Z). Egg–N2 stages stay within the top 40 m during both day and night, while feeding nauplii (N3–N6) and young copepodids (C1–C2) remain at the depth of chlorophyll maximum. For active individuals stages C3–C6 in open water regions, we simulate size-dependent diel vertical migrations (e.g. Daase et al., 2008; Ohman and Romagnan, 2016) similar to the *C. finmarchicus* IBM, by estimating the day depth (DZ) as a function of individual size (S):

$$DZ = VM_1 + VM_2 \times S \quad (1)$$

where VM_1 and VM_2 are constants (Table 4), and S is estimated from the structural weight (SW) and lipid content (L):

$$S = 0.001x0.7(SW + L)^{0.278} \quad (2)$$

At night, C3–C6 remain at the depth of chlorophyll maximum. In regions with sea-ice, C3–C6 remain at the surface both day and night to graze on ice-algae (see below).

Compupods may overwinter from stage C3 (Daase et al., 2013; IMR unpublished data; Wold et al., 2011), though whether they complete the first winter as C3 or C4 depends on growth during the preceding spring and summer. Phenology is in the model driven both by internal state (Fiksen and Carlotti, 1998) and genes (Fiksen, 2000), and seasonal descent will occur when i) a compupod has sufficient lipid reserves to sustain respiration when overwintering, and ii) day of year ≥ EDD. Similar to the *C. finmarchicus* IBM, compupods move at a speed of 2 m h^{-1} during seasonal migrations and remain at the overwintering depth or the bottom (whichever the shallower) until the wake-up day.

Horizontal movement simulates passive drift with ocean currents based on the (X, Y, Z) position of the compupod, calculated using velocity fields from the ROMS model with a classic, 4th order Runge-Kutta algorithm. The horizontal movement also includes a random component representing sub-grid diffusion processes.

Growth. Embryonic development (egg–N2) follow the Bêlehrádek temperature function (Corkett et al., 1986), here parametrized for egg and nauplii *C. glacialis* reared in laboratory at 0 °C under satiated food

Table 4
Model parameters of the *Calanus glacialis* individual based model (IBM) in the Barents Sea.

Parameter	Value	Unit	Reference
Egg stage longevity (Eq. 3)	1215	wd	Jung-Madsen and Nielsen (2015)
N1 "	1621	"	"
N2 "	1255	"	"
N3 molting weight	0.195	µg C	Bailey et al. (2017) (mean)
N4 "	0.541	"	"
N5 "	1.14	"	"
N6 "	1.93	"	"
C1 "	3	"	Slagstad and Tande (1990)
C2 "	6.5	"	"
C3 "	12	"	"
C4 "	55	"	"
C5 "	390	"	"
C6 "	474	"	"
Egg stage-dependent mortality	0.25	d^{-1}	
N1–N2 "	0.15	"	
N3–C2 "	0.05	"	
C3–C6 "	0	"	
Minimum structural spawning weight	237	µg C	(50 % of C6 molting weight)
Egg weight	0.4	µg C	Hirche (1989)
Egg lipid content	0.2	"	(50 % of egg weight)
Clutch size	15	d^{-1}	Hirche and Bohrer (1987)
Maximum number of eggs	1200	$female^{-1}$	Hirche (1989)
α (Eqs. 4 and 5)	0.8	wd	Carlotti and Wolf (1998); Campbell et al. (2009)
Q_{10} (Eq. 4)	1.5	wd	Grote et al. (2015) (temp. 0–5 °C)
Imax, stages N3–C4 (Eq. 4)	0.3	d^{-1}	Campbell et al. (2016)
Imax, stages C5–C6 (Eq. 4)	0.12	"	"
b, stages N3–C4 (Eq. 4)	15	wd	Huse et al. (2018) *
b, stages C5–C6 (Eq. 4)	30	"	"
Assimilation efficiency (λ)	0.2	"	Slagstad and Tande (1990)
QR_{10} (Eq. 5)	2.13	"	"
r_1 (Eq. 5)	0.01/24	"	Carlotti and Wolf (1998)
r_2 (Eq. 5)	0.2	"	Carlotti and Wolf (1998)
Overwintering metabolism	0.1	% *sweight* d^{-1}	Fiksen (2000)
VM_1 (Eq. 1)	13	wd	Huse et al. (2018) *
VM_2 (Eq. 1)	20,500	"	"
ice_{crit} (critical ice-cover for ice-algae)	0.1	"	
$angle_{crit}$ (critical solar angle for ice-algae)	−5	°	(~onset of civil twilight)
$IceAlgae_{max}$ (Eq. 7)	100	mg C m^{-2}	(only available in surface layer)
$bloom_{days}$ (Eq. 7)	21	wd	
Ice algae cutoff day	200	"	(mid-June)

wd: without dimension, *taken from *C. finmarchicus* IBM; *sweight*: structural weight, d: day.

conditions (Jung-Madsen and Nielsen, 2015):

$$D_j = a_j(T + 15.7)^{-2.05} \quad (3)$$

where D_j is the duration (days) of stage j, a_j is a stage-specific parameter (Table 4) and T is temperature in °C. As for *C. glacialis* in nature (Daase et al., 2011; Jung-Madsen and Nielsen, 2015), we let feeding commence at the third nauplii stage after which individual growth is estimated using a bioenergetic growth model adopted from Carlotti and Wolf (1998). Ingestion is calculated as a function of size (*sweight*), temperature and ambient food:

$$I = I_{max}(Q_{10})^{T/10} sweight^{a} \frac{\max(0, food - thres)}{b + \max(0, food - thres)} \quad (4)$$

where I_{max}, Q_{10}, a and b are constants and *food* is the ambient food availability. To avoid the phyto- and microzooplankton fields from becoming locally extinct, minimum concentration thresholds (*thres*) set to 0.1 mg N m^{-3} for each food source is not available for grazing. This is a purely technical solution which we compensate for with a constant, low-concentration background food field of 0.3 N m^{-3}. Ingestion rates in *C. glacialis* follow allometric theory and are lower for the older copepodids (C5) and adult stage (Campbell et al., 2016), so we employ different maximum ingestion rates (*Imax*) and functional response constants (*b*) for stages N3–C4 compared to C5–C6 (Table 4).

Similar to Carlotti and Wolf (1998) we set egestion (E) to a constant proportion of ingestion (λI) and split respiration into basic and active metabolism, where the basic part is a function of size and temperature and the active part is a constant fraction (r_2) of the ingestion:

$$R = r_1 sweight^{a} QR_{10}{}^{T/10} + r_2 I \quad (5)$$

Growth then emerges as total ingestion minus egestion and respiration:

$$G = I - E - R \quad (6)$$

Stages N3–C2 invest growth into structural weight, while stages C3-C6 invest growth into both structural weight and lipids at a ratio defined by the allocation-to-soma ratio (Table 2). Compupods will change stage when a stage-specific molting weight is reached (Table 4) at a moulting cost of 10 % of the structural weight. If metabolic expenditure exceeds ingested carbon, the lipid reserves are drained before the structural weight is affected. When in diapause, compupods cease feeding and a resting metabolism of 0.1 % *sweight* d^{-1} is assumed (Carlotti and Wolf, 1998; Fiksen, 2000).

Food sources. *C. glacialis* is not strictly herbivore, although pelagic algae tend to dominate the diet during phytoplankton blooms and ice-algae are considered important in areas with sea ice (Cleary et al., 2017; Søreide et al., 2010, 2008). In the IBM, compupods feed on phyto- and microzooplankton fields from the NPZD, and we have also added an "ice-algae" food source developed for the *C. glacialis* IBM. The current understanding of ice-algae bloom phenology is incomplete, but light is considered key for bloom initiation in early spring and bloom termination is thought to be driven by nutrient depletion in summer (Leu et al., 2015 and references therein). In our model we make ice-algae available as food during periods when the sun height at noon reaches above a critical level ($angle_{crit}$) in areas with sea ice. Daily ice-algae concentration is estimated as a function of ice-cover and will build up gradually during a "pre-bloom" phase:

$$p\_IceAlgae_d = (p\_IceAlgae_{d-1} + \frac{IceAlgae_{max}}{bloom_{days}}) \quad (7)$$

until $p\_IceAlgae_d = IceAlgae_{max}$, where $IceAlgae_{max}$ and $bloom_{days}$ are constants for the maximum ice-algae concentration and the length (in days) of the pree-bloom phase. After that, $p\_IceAlgae_d = IceAlgae_{max}$. We set $IceAlgae_{max}$ at 100 mg carbon m^{-2}, which we consider a conservative estimate for this region (Tamelander et al., 2009). After reaching $IceAlgae_{max}$, the concentration is only adjusted by *ice* until $ice < ice_{crit}$ or a fixed date is reached (Table 4). When the local ice-concentration in the grid cell is above 10 % (ice_{crit}), the ice-algae concentration is computed as:

$$IceAlgae = ice \times p\_IceAlgae_d \quad (8)$$

where *ice* is the fraction (0–1) of the grid cell covered by ice. Where ice is below 10 %, the ice-algae concentration is set to zero.

Feeding in the IBM is non-selective, and consumption is estimated according to the relative proportion of each food source (phytoplankton, microzooplankton, ice-algae) in the modelled environment.

Mortality. Young stages (egg–C2) suffer instantaneous mortality rates which decline with compupod stage (Table 4) (e.g. Aksnes and Blindheim, 1996). For older stages C3+, mortality is assumed to largely result from visual and tactile predation, spawning stress and starvation (e.g. Daase and Søreide, 2021).

Both visual and tactile predation is estimated as in the *C. finmarchicus* IBM described in Huse et al. (2018), largely based on the work by Aksnes and Utne (1997). Briefly, the visual predation is a function of compupod size, ambient light and (assumed) pelagic fish visual capacity and decreases with depth as light attenuates in the water column. Here we also reduce the estimated visual predation risk with increasing ice cover, from maximum risk at $ice = 0$ to zero when $ice = 1$, to capture the effect of ice impeding surface irradiation reaching the water column (Varpe et al., 2015). Tactile predation is a function of predator search range and swimming velocity, hence independent of light.

Starvation is also based on the *C. finmarchicus* IBM, and compupods will suffer starvation mortality when their total weight (lipids + structural weight) drops below 92 % of the stage-specific molting weight (the minimum weight for a given stage).

The total mortality rate is adjusted based on population size, simulating density-dependent processes and to better fit with observed population densities. For this, we estimate a mortality correction factor C_{mort} on January 1 each year which serves to adjust the mortality rates until January 1 the following year. The correction factor follows a log-like function:

$$C_{mort} = (0.0738 + 0.5\left(1 + \frac{1}{B} \times ln\frac{A}{1-A}\right)) \times (C_{max} - C_{min}) + C_{min} \quad (8)$$

where $C_{max} = 1.4$ and $C_{min} = 0.6$, $B = 4.59512$ and A is a function of the total biomass on January 1 and an assumed long-term mean *C. glacialis* standing stock of 1.5 MT (see section 2.2.5).

Mortality is implemented as a reduction in the internal number of the superindividual, and when $inumb \leq 1$ the compupod is removed from the model population. Compupods are taken out directly when spawning the maximum number of eggs (Table 4), if advected out of the model domain, and at stage C6 if the given sex is "male". Furthermore, compupods drifting into the Norwegian and Greenland Seas suffer an additional mortality rate of 0.01 d^{-1} based on the low abundances observed from these areas (Broms et al., 2009; Choquet et al., 2017; Strand et al., 2020) (but see Discussion).

Reproduction. Spawning is initiated once a day (midnight), and adult females may spawn as long as they are above 100 m depth (surface spawning; Madsen et al., 2001), their structural weight is above a critical level and they have sufficient lipid reserves to lay a minimum of one clutch of eggs (Table 4). Accumulated lipids determine the total number of eggs a compupod may produce, which is the lipid reserves divided by the egg weight. For each spawning event one new superindividual compupod is produced, representing a total number of identical siblings given by:

$$Inumb = (parent\ \ inumb) \times \frac{parent\ \ lipid\ \ reserve}{eggweight}$$

3. Results

3.1. Spatial distribution

From the initial *C. glacialis* compupod population released in the northern Barents Sea (Fig. 1), the population is over time spread out to cover a fairly large region (Fig. 2A). Additional mortality rates are necessary for compupods in the Norwegian Sea (section 2.2.7 *Mortality*) to prevent a population establishing there. Biomass varies spatially from below 1 mg C m^{-3} to over 5 mg C m^{-3}. Regions with high biomass m^{-3} are characterized by strong flow (currents shown in Appendix Figs. A4 and A5), such as the northern Barents Sea shelf break and the St. Anna Through. Biomass is also retained in the northern Barents Sea where currents are weaker and there appears to be some kind of local retention mechanism. Compupods advected out of the Barents Sea south of Spitsbergen are carried northwards with strong currents, which are partly deflected eastwards north of Spitsbergen. Here, compupods may re-enter the Barents Sea through the opening east of Spitsbergen or around the east side of Franz Josefs Land. Compupods advected out of the Barents Sea through the easternmost opening (between Franz Josefs Land and Novaya Zemlya) will be transported into the Kara Sea, or towards the Arctic Ocean with strong currents in the St. Anna Through.

Using output from the *C. finmarchicus* IBM we have estimated the biomass-ratio between *C. glacialis* and *C. finmarchicus* as (carbon_*glacialis* – carbon_*finmarchicus*)/(carbon_*glacialis* + carbon_*finmarchicus*). With this, we get a spatial distribution of the two species in the model domain ranging from 1 (all *C. glacialis*) to −1 (all *C. finmarchicus*) (Fig. 2B). There is a clear separation between these two species in the Barents Sea, with *C. glacialis* dominating in the north and *C. finmarchicus* in the south-west, south and east. There is co-existence between the two in most of the Barents Sea, but the presence of *C. glacialis* in the south and east is overshadowed by the high biomass of *C. finmarchicus* in these regions (Fig. 2A and B).

3.2. Seasonal biomass dynamics

Modelled population biomass fluctuates over the season, with a mean seasonal minimum of 1.06 million tonnes (MT) carbon and a mean maximum of 5.16 MT carbon (Fig. 3). The seasonal fluctuations are relatively stable over the 25 basic simulation runs, and the mean biomass over a season is not strongly correlated with the starting biomass (January 1) of each model run (Pearson correlation, r = 0.48, p = 0.0141). Young stages (C1 to C3) have the largest seasonal fluctuations in abundance, while C4 and C5 have more stable abundances over a season (Appendix Fig. A1).

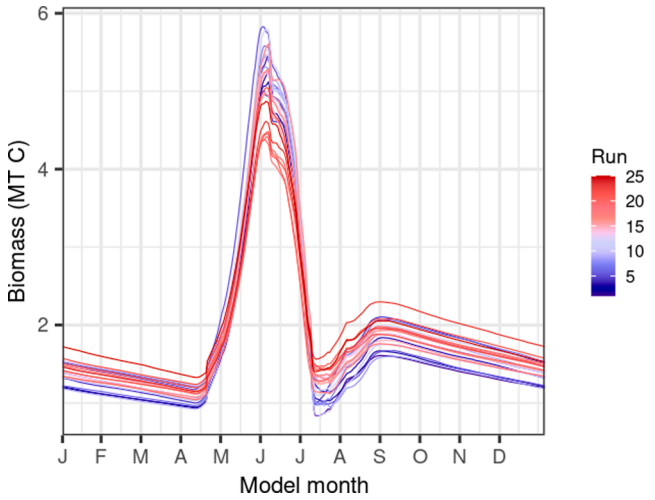

Fig. 3. Seasonal development of population biomass (million tonnes carbon) modelled over the 25 basic simulation runs (colors).

Eggs start appearing from late April, but the peak egg production occurs in early July (Fig. 4). Development from eggs to C1 takes around one month, and biomass of both C1 and C2 peak in August. The new generation of compupods largely reaches stage C3 in August–September (but some already in June–July), and during winter C3 comprises almost half of the total population biomass while the rest consists of stages C4 and C5 (Fig. 4, see also biomass ratios in Appendix Fig. A2).

The seasonal buildup of maximum population biomass (May–June, Fig. 3) corresponds to the seasonal biomass-peaks of stages C4 and C5 (Fig. 4). Biomass of stage C4 starts increasing in late April/early May with the development of C3 from the overwintering population into C4. The biomass of C4 builds up gradually over the course of a month, after which it declines when most copepodids have advanced into C5. Biomass of C5 peaks in June, about two weeks after the peak of C4. Adults (stage C6) are not a major part of the overwintering population but start appearing in late April – May and peak in biomass around two weeks later than C5. At this time (June–July) the population largely

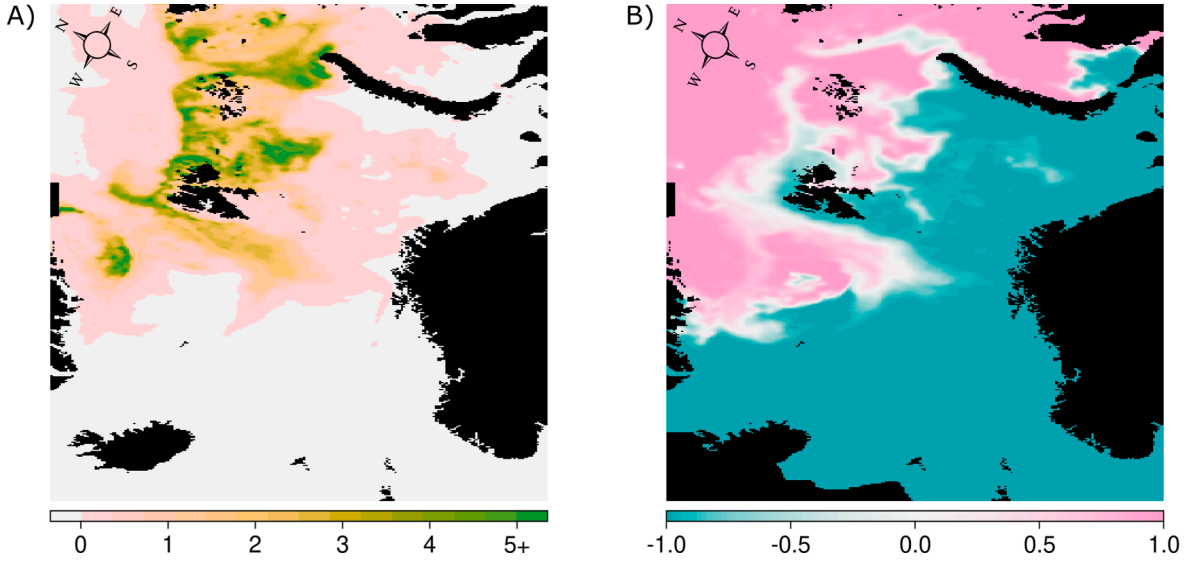

Fig. 2. A) Spatial distribution of modelled *C. glacialis* biomass (mg C m^{-3}), and B) ratio between *C. glacialis* (1, pink) and *C. finmarchicus* (-1, turquoise) in the NORWECOM.E2E model domain. Both panels display means over the 25 basic simulation runs.

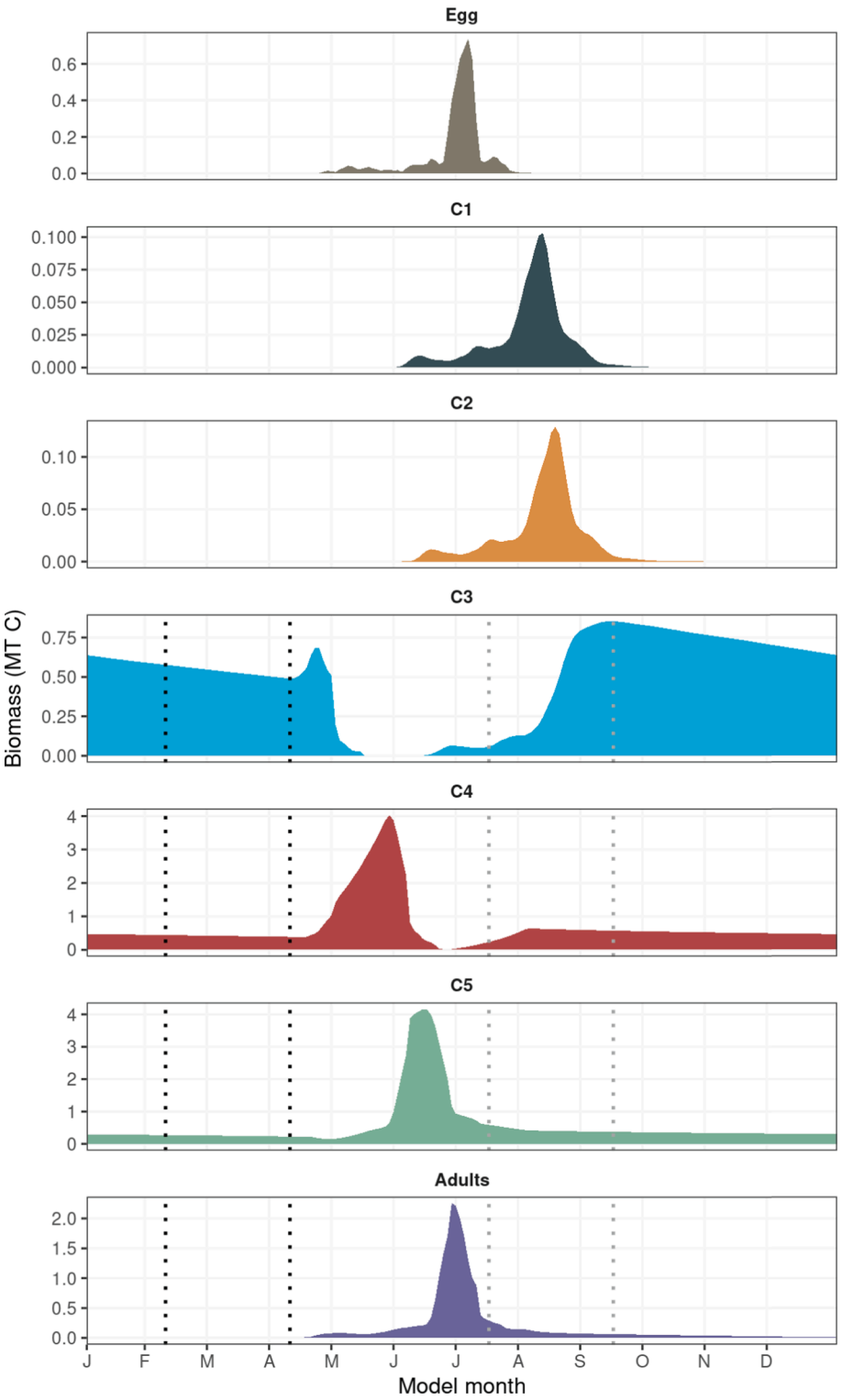

Fig. 4. Seasonal, stage-specific biomass development (million tonnes carbon) of modelled *C. glacialis* compupods, as means over the 25 basic simulation runs. Dotted lines refer to the time-intervals of the seasonal vertical migrations for stages that may overwinter; ascent from diapause (black lines) between day 40–100, and descent (grey lines) to diapause between days 196– 256 (see Table 2).

consists of stages C5 and C6 in terms of biomass (Fig. 4 and Appendix Fig. A2). A second increment in C4 biomass is seen at the later end of the growth season (July–August) when some C3 of the new generation advances into C4. Stages C4 and C5 dominate the population biomass from May throughout the summer until September, except for the small period in summer when adults peak in biomass and C5–C6 dominates. The total biomass has two seasonal minimums (Fig. 3), one at the transition between the overwintering phase and the growth season (March–April) and a second after the peak in adult biomass when the new generation is spawned (July).

3.3. Seasonal trophic interactions

Phytoplankton production is in the model limited to open (ice-free)

waters. The spring bloom starts in the southern Barents Sea in April, and advances northwards during May–July with the retreating sea-ice (Fig. 5, ice-extent is provided in Appendix Fig. A3). There are two seasonal peaks in phytoplankton consumption by the compupod population, one in late May/early June and a second peak about two months later (Fig. 6). We interpret the first peak to be associated with grazing by the population south and east of Spitsbergen where there are open waters in spring. The northernmost part of the population is covered by ice until July–August and presumably drives the second peak when they get access to phytoplankton as the sea ice retreats. Annual consumption of microzooplankton is about one order of magnitude lower than the total grazing of phytoplankton (0.48 MT carbon *versus* 4.77 MT carbon, respectively, mean over the basic simulation runs). Consumption of ice-algae is, on the other hand, comparable to the total grazing on phytoplankton (annual mean of 5.52 MT carbon). Ice-algae become available as food for compupods when the solar angle at noon is greater than −5° (Table 4), hence earlier in the season in the southernmost ice-covered regions (e.g. Appendix Fig. A6), and ice-algae consumption by the compupods commences in April (Fig. 6). The peak ice-algae consumption coincides with the time of the first peak in phytoplankton grazing, after which it drops with the retreating sea-ice. Both ice-algae and phytoplankton consumption fuel maturation of compupods from the overwintering population and the following peak in egg production occuring around one month after peaks in ice-algae and phytoplankton consumption (Fig. 6). The second peak in phytoplankton consumption (and predation on microzooplankton) fuels growth of nauplii and young copepodids into C3, and accumulation of lipid reserves for overwintering stages (C3–C5) before descending to diapause.

Visual predation is the dominant mortality cause for compupods early in the season, and the total consumption by predators increases with the build up of C4–C6 biomass. Visual predation drops gradually

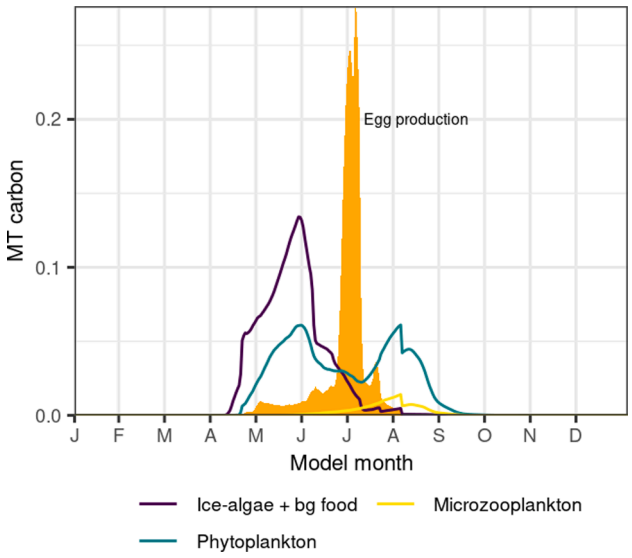

Fig. 6. Seasonal consumption by the *C. glacialis* population of the three available food sources in the model: ice-algae (including background food field, see Section 2.2.7 *Growth*), phytoplankton and microzooplankton. Values are in million tonnes carbon, as mean per day of year over the 25 basic simulation runs. The orange area displays mean egg production over the same period.

when the new generation is spawned ("spawned out" mortality for stage C6, Fig. 7) and the compupod population is dominated by smaller sized individuals. The total loss to tactile predation is 40 % of the loss to visual predation over a season (1.01 *versus* 2.53 MT carbon, respectively, mean over the basic simulation runs). Mortality loss from starvation is

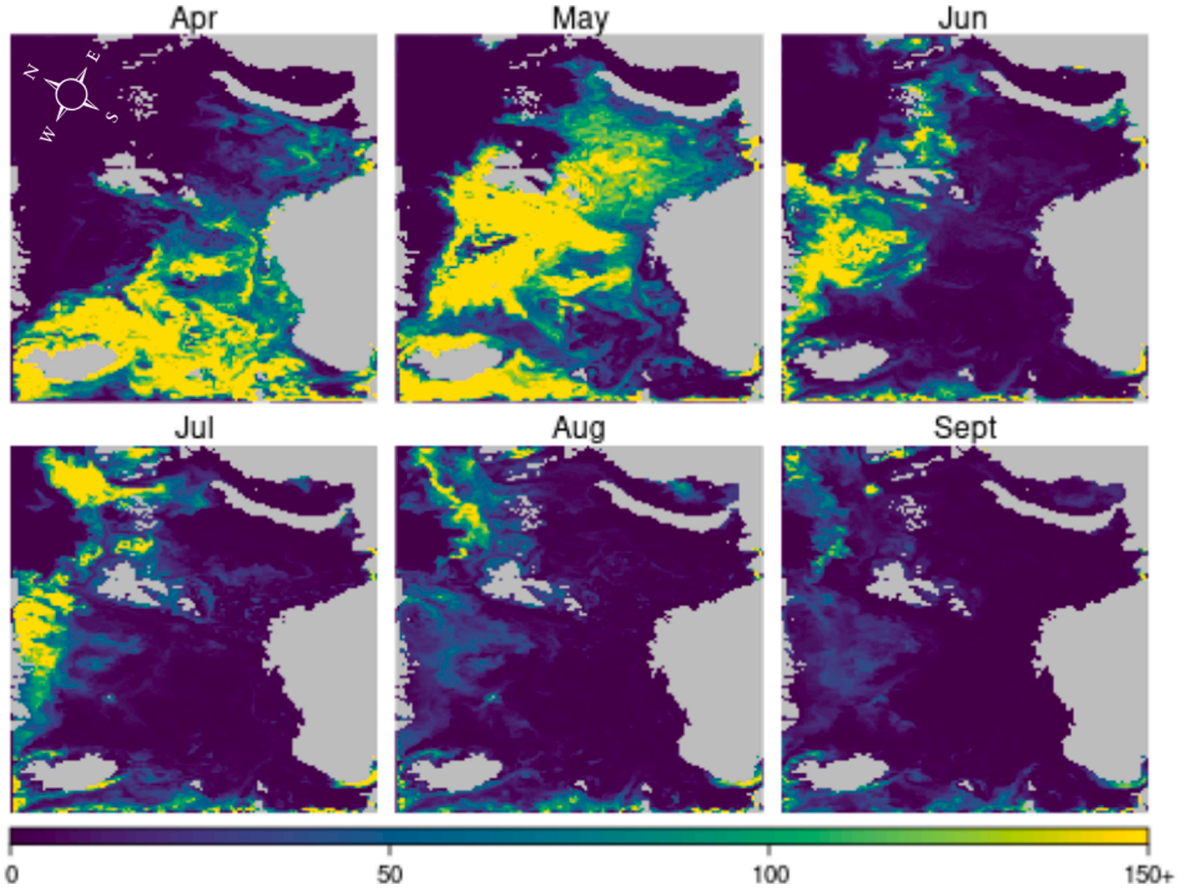

Fig. 5. Modelled monthly (accumulated) phytoplankton biomass (mg C m^{-3}) at 50 m depth during one growth season (first basic simulation year).

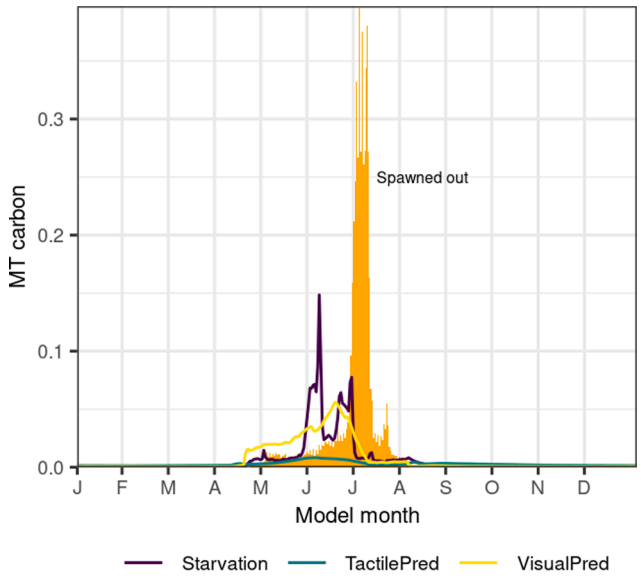

Fig. 7. Seasonal mortality losses from starvation, tactile predation and visual predation of the modelled *C. glacialis* population. Values are given in million tonnes carbon, as means per time step over the basic simulation runs. The orange area in the background displays mean mortality from spawning stress over the same period. One high value of spawning mortality (0.56 MT carbon, day 190, mid June) was excluded from the figure.

comparable to mortality from visual predation (mean 2.4 MT carbon), and surpasses loss from visual predation in early June when the ice-algae and phytoplankton consumption start declining (Figs. 6 and 7). A second peak in starvation loss occurs around the time of peak adult biomass (late June). Overall, mortality after spawning of C6 is the major mortality cause at a total of 4.82 MT carbon in mean over a season.

3.4. Development

The median number of days to develop from egg to stage C3 is 53 days for our modelled *C. glacialis* compupods (Table 5), though the individual variability is high (mean 66 days, SD 38 days). Since C3 is the main overwintering stage, it takes a median of 300 days for a compupod to reach stage C4, after which the development up to the adult stage is faster (36 additional days to C5 and 20 more days to reach C6, in median estimates). Many compupods are able to complete their life cycle with only one diapause, but around 30 % require two years to reach the adult stage. Common for compupods with a 2-years life cycle is that more time has been spent in northern parts of the model domain (north of 77°N), particularly from eggs to C4 (Fig. 8). For comparison, the modelled *C. finmarchicus* compupods spend a median of 21 days to reach stage C3, and 57 days to stage C6 (Table 5). Modelled *C. finmarchicus* compupods have smaller critical moulting weights (minimum weight to reach a given stage) compared to the *C. glacialis* model presented here (Table 4, Huse et al. 2018). However, the critical weight for adult *C. finmarchicus*

Table 5
Development time (days to reach the given stage) for the modelled *C. glacialis* and *C. finmarchicus* populations.

Species	Stage	Median	Mean	SD
C. glacialis	C3	53	66	38
	C4	300	289	50
	C5	336	337	17
	C6	356	363	43
C. finmarchicus	C3	21	30	24
	C4	31	43	34
	C5	38	57	48
	C6	57	139	114

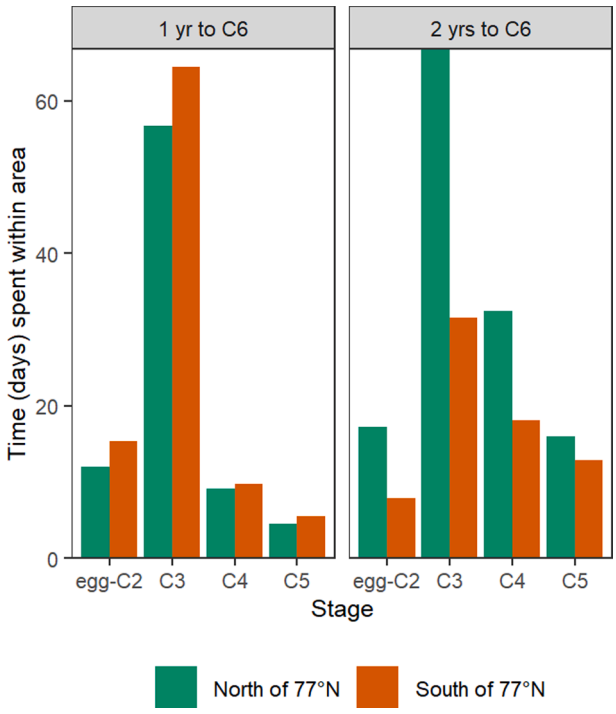

Fig. 8. Mean number of days spent north and south of 77°N for *C. glacialis* compupods with a 1 (left panel) and 2 (right panel) years life cycle, estimated over the 25 basic simulation runs.

(90 μg C, Huse et al. 2018) is considerably higher than the critical weight for C3 *C. glacialis* (12 μg C, Table 4) so *C. finmarchicus* also develops faster than *C. glacialis* in this model system, presumably due to different temperature regimes in the regions where they dominate (Fig. 2B, Appendix Fig. A7).

4. Discussion

Coupling zooplankton models with modelled ocean circulation and primary production enables new insight difficult to obtain from *in situ* observational studies alone. We developed an IBM of the Barents Sea *C. glacialis* population to study their seasonal development and spatial distribution under the forces of advection and environmental variation. Water temperature, sea-ice extent and timing of food availability varied greatly between northern and southern parts of the model domain, influencing copepod development in the modelled population (i.e. compupods). The model indicated two seasonal peaks in phytoplankton consumption by the compupod population, the first in open waters in May–June when the population biomass was dominated by older stages C4–adults. Together with ice-algae consumption this fuelled the maturation of the overwintering population. A second peak in phytoplankton consumption coincided with ice retreat in northern regions (July–August) after the peak in egg production and corresponding with the development of the new generation. The seasonal buildup of biomass in stages C4 and C5 contributed to a maximum of population biomass between May and July, while seasonal minimums in biomass were associated with the winter-spring transition (February–April) and the spawning of a new generation (July). The model indicated a clear separation between *C. glacialis* and *C. finmarchicus* in the Barents Sea, with *C. glacialis* dominating in the north and *C. finmarchicus* in the south-west, south and east.

4.1. Model strengths and weaknesses

The applied model is founded on present knowledge of *C. glacialis* ecology and biology, but is still a coarse approximation of a complex

reality. Integrating existing knowledge into this type of model framework is important for knowledge validation and improved understanding of complex processes (Aarflot et al., 2022). A key strength of our model is the focus on individuals. Hence, the population properties are not predefined but an emergent outcome from our simulations. Furthermore, by coupling to published models of ocean circulation and primary production we explore how the spatial and seasonal dynamics of this species is structured by bottom-up forcings from the environment. This complexity is, however, also a weakness since it hampers sensitivity testing of model parameters due to the model's computational constraints. Hjøllo et al. (2012) evaluated sensitivity of the *C. finmarchicus* IBM to the number of superindividuals used in simulations, and suggested that 50.000 SI was suitable for representing dynamics of this species in the Norwegian Sea. The present set-up typically had 20.000–30.000 active superindividuals of *C. glacialis*, though a simple sensitivity-test with quadroupling the number of superindividuals did not change the modelled spatial distribution (Appendix Fig. A8).

C. glacialis spends part of the year diapausing at depths, and what triggers the descent and ascent is still poorly known. The onset of diapause was here implemented to occur after a random day under the constraint that enough fat reserves had been built (EDD gene), complying with the "lipid accumulation window" hypothesis (Baumgartner and Tarrant, 2017). This process is nevertheless not fully understood, and there are more C3 in our modeled overwintering population than we expected based on earlier records from this region (Melle and Skjoldal, 1998). Later descent would allow more compupods to develop into C4 before overwintering, and rules determining entry to and exit from diapause should be further examined in future development of the model. Dominance of C3 abundance in the overwintering population does, however, comply with recent findings during the Nansen Legacy project (A. Wold *pers. comm.*) and with stage-structured data on *C. glacialis* from a joint Norwegian-Russian monitoring survey in 2013 (Fig. 9).

Low contribution of adults to the total population biomass may be a model artifact based on how the spawning and overwintering processes have been parametrized. A female compupod will start spawning when having aqcuired sufficient lipid reserves and continue until the reserves are drained. Potential environmental cues for commencing or delaying the spawning process are not considered. Also, ontogenic development is dependent on food intake and will hence cease when compupods enter the overwintering phase. Enhanced knowledge on factors regulating spawning, other than fat reserves, and whether ontogenic development is possible when in diapause, will be useful for evaluating the realism of the processes in our *C. glacialis* IBM.

At the population level, *in situ* mortality rates and their causes are impossible to measure thus a balancing between reproduction, growth and longevity with the different mortality terms is necessary for these types of models. The area-dependent mortality added to avoid a build-up of a *C.glacialis* population in the Norwegian Sea, is an example where knowledge gaps on the controling mechanism are met with an *ad-hoc* model formulation. These can, however, also be used for posing new hypotheses (see below).

4.2. Spatial distribution

The spatial divide between a *C. glacialis* domain in the northern Barents Sea and dominance of *C. finmarchicus* in the west, south-west and east agrees with in-situ observations (Aarflot et al., 2018; Arashkevich et al., 2002; Hirche and Kosobokova, 2003). This separation appears to be structured by ocean circulation and fits well with the circulation pathways for Arctic and Atlantic waters in Fig. 1. *C. finmarchicus* is advected into the Barents Sea from a source population in the Norwegian Sea basins (Skjoldal et al., 1992) and dominates in biomass in Atlantic water masses (Fig. 1, Aarflot et al., 2018). Hirche and Kosobokova (2003) demonstrated increasing dominance of *C. glacialis* moving northwards in the Barents Sea, supported by its

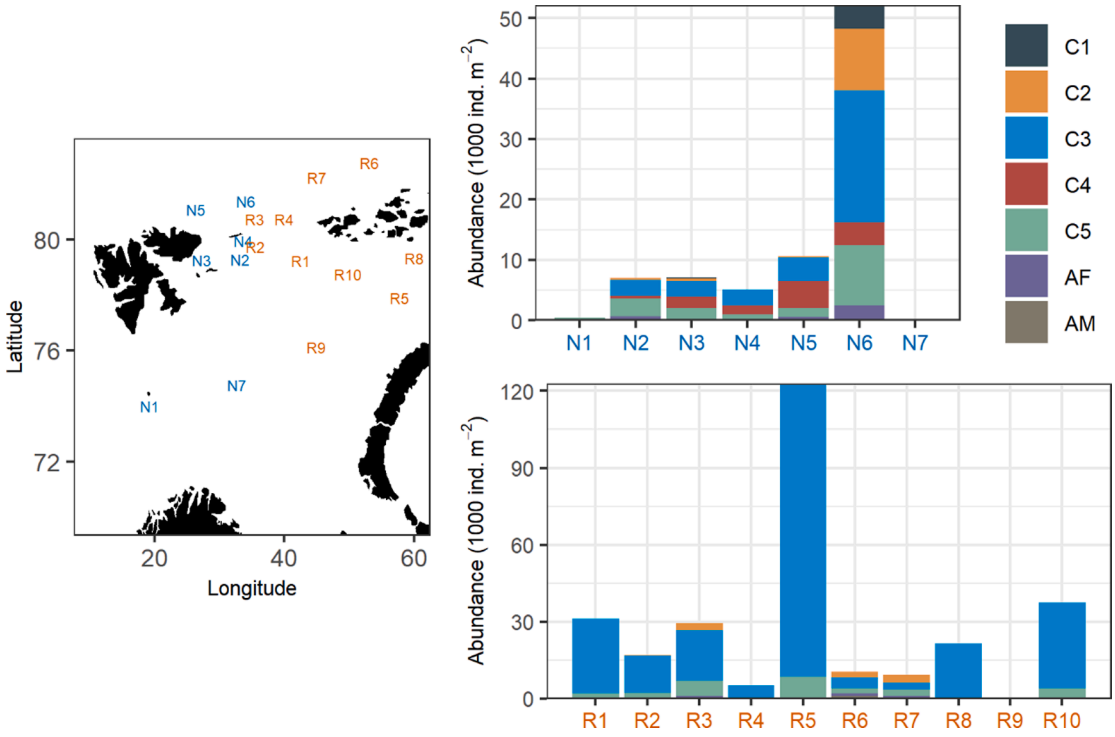

Fig. 9. *Calanus glacialis* abundance by stage, from a joint Norwegian-Russian monitoring survey in 2013. The top-right panel shows Norwegian (Institute of Marine Research, IMR) data from WP2 samples (180 μm mesh size) taken between August 16th and September 19th, and the bottom-right panel displays Russian (Polar Branch of FSBSI "VNIRO" ("PINRO" named after N.M. Knipovich)) data taken with a Juday net (similar mesh size) collected between September 20th and October 20th. The map (left panel) shows the location of the sampling stations referred to in the x-axis of the right panels (N = Norwegian, R = Russian). Very low abundances were sampled at stations N1 (C5 copepods), N7 (C5 copepods) and R9 (C3 and C5 copepods).

dominance in Arctic waters in Aarflot et al. (2018). Our results show that *C. glacialis* will also be transported to more southern regions of the Barents Sea, though in considerably lower densities than *C. finmarchicus*. This agrees with earlier observations of *C. glacialis* in the south-eastern and eastern Barents Sea during late summer-early autumn, but in low abundances with high interannual variability (ICES, 2021; Orlova et al., 2011).

Core populations for drifters like zooplankton are dependent on circulation loops or similar advective forces that enable retention and life cycle closure within a specific area. While the Norwegian Basin and Lofoten Basin Gyres retain a population of *C. finmarchicus* in the Norwegian Sea (Søiland and Huse, 2012), the source of *C. glacialis* in the highly advective Barents Sea is, to our knowledge, still an open question. The model indicated local circulation loops maintaining high *C. glacialis* densities in the northern Barents Sea (see also Loeng, 1991), however it is not clear whether these are sufficiently persistent to retain a population in this region over multiple years. Recirculation of individuals around Svalbard or east of Franz Josefs Land is another potential mechanism retaining *C. glacialis* in the northern Barents Sea. A particle drift study showed that polar cod eggs and larvae from the east of Svalbard will be retained into the northern Barents Sea due to clockwise drift around the Svalbard archipelago (Eriksen et al., 2019; Huserbråten et al., 2019). There is also a possibility that *C. glacialis* in the Barents Sea is maintained by supply from a source population elsewhere, which has not been considered here. For instance, recent studies have shown a core population of *C. glacialis* centering around the outer shelf and slope of the Arctic Ocean (Ershova et al., 2021) contrary to earlier descriptions of *C. glacialis* as a "neritic" (shelf-associated) species (Jaschnov, 1970). Also, high genetic similarity between *C. glacialis* populations in the Arctic has been suggested (Weydmann et al., 2016). The source of *C. glacialis* in the Barents Sea remains a central, unresolved question to address with our model system presented here.

The role of top-down control in structuring *C. glacialis* spatial distribution is a missing component in our model. High abundance and energy content of *Calanus* spp. makes them valuable food for local predators such as larger carnivorous zooplankton (Falk-Petersen et al., 2002, 2000a), sympagic amphipods like *Gammarus wilkitzkii* (Scott et al., 2001) and Arctic pelagic fish such as polar cod (Orlova et al., 2009). It is also important food for migrating predators such as the pelagic fish capelin and herring (Huse and Toresen, 1996; Orlova et al., 2009) and seabirds feeding on *Calanus* (Karnovsky et al., 2003; Steen et al., 2007). Earlier studies have suggested strong top-down control from predators on zooplankton in the Barents Sea (Stige et al., 2014), and that the magnitude of the control is likely driven by spatial variation in bathymetry (Aarflot et al., 2020). Due to this, our results are not expected to perfectly match with *in situ* observations of *C. glacialis* abundance, but rather demonstrate where the copepods will be transported and may survive given the prevailing environmental conditions. Additional mortalities were necessary for compupods advected into the Norwegian Sea, where *in situ* studies have reported negligible abundances of *C. glacialis* (Broms et al., 2009). Low abundances in this region cannot be explained by environmental conditions given that it is capable of sustaining local populations in several Norwegian fjords (Choquet et al., 2017; Niehoff and Hirche, 2005). High predation pressure from size-selective predators may therefore be central for suppressing *C. glacialis* abundances in the Norwegian Sea, similar to what has recently been suggested for the larger congener *C. hyperboreus* (Aarflot et al., 2022).

4.3. Seasonal development

Modelled population biomass fluctuates over the season, with a maximum peak at 5 times higher carbon mass than the seasonal minimums. Biomass fluctuations are to a large degree driven by stages C4 and C5, which have been shown to make the largest contribution to the biomass also from empirical studies (Aarflot et al., 2018). A large proportion of *C. glacialis* in the Barents Sea should be able to complete their life-cycle with only one diapause phase, and a common feature for compupods with a 2-years life cycle was that more time had been spent in northern parts of the model domain (north of 77°N) where temperatures are colder and primary production is delayed compared to the south. Melle and Skjoldal (1998) also observed a higher fraction of *C. glacialis* with a 2 year life-cycle in polar regions of the Barents Sea compared to Atlantic water regions.

Egg production in our model population started in May and reached a maximum peak in early July. According to Falk-Petersen et al. (2009), *C. glacialis* can be found spawning from April until the end of August, and young stages (C1-C3) comprised up to 75 % in abundance of a population sampled across the marginal ice-zone in the Barents Sea in July (Arashkevich et al., 2002). Data from a joint Norwegian-Russian monitoring survey in 2013 (Fig. 9) show that stages C1-C3 are abundant in samples from the northern Barents Sea collected between mid-August to mid-September, and that C3 dominate in abundance in the north-eastern regions between late September and late October. Also, recent field campaigns from northern parts of the Barents Sea have sampled *Calanus* spp. nauplii in July (A. Wold *pers comm.*) and C1-C3 in August and September (A. Wold *pers comm.*, I. Prokopchuk *pers. comm.*). In sum, this supports a prolonged period of reproduction for *C. glacialis* over the summer in the Barents Sea ecosystem.

The peak egg production rate often corresponds with high pelagic chlorophyll-*a* concentration later in the season (Hirche and Bohrer, 1987; Hirche and Kwasniewski, 1997; Tande et al., 1985). Laboratory experiments have demonstrated that *C. glacialis* females are able to conserve their reproductive capacity for at least 7 months (Hirche, 1989), and they respond fast when food becomes available (Hirche, 1989; Madsen et al., 2008). This indicates a spawning potential for *C. glacialis* that is driven by the environmental conditions. The Barents Sea experienced a cold period during 1980, warming between 1990 and early 2000th, and a record warm condition in 2016 (ICES, 2021; Ingvaldsen et al., 2021). Dalpadado et al. (2020) showed that since 1990 the timing of peak spring phytoplankton bloom in northern BS has advanced by a month and phytoplankton production almost doubled. These changes may influence the timing of *C. glacialis* spawning and feeding conditions. The differences between the model results and earlier observations in the 1980–1990 s (Hirche and Kosobokova, 2003; e.g. Melle and Skjoldal, 1998) suggesting earlier peak of egg production could be related to different environmental conditions and different temporal and spatial coverage between the model and *in situ* studies.

The modelled overwintering population was dominated in abundance by copepodid 3, which is supported by the Norwegian-Russian monitoring data from 2013 (Fig. 9) and unpublished data from the recent Nansen Legacy field campaigns (A. Wold, *pers. comm.*). Dominance of C3 in the overwintering population means that maturation of adults the subsequent spring will be delayed as C3 require about two months to reach the adult stage. Individual development rates from egg to C3 in our model (median 53 days) are reasonable given earlier publications by Jung-Madsen et al. (2015; 52 days from egg to C1) and Ji et al. (2012; 54 days from egg to C3). Studies from Amundsen Gulf in 2007–08 showed that *C. glacialis* overwintered mainly as C3 and C4 (Wold et al., 2011), suggesting a delayed development where only part of the population manages to spawn in spring, while the rest of the overwintering population starts to spawn later in summer or the subsequent year. Whether a compupod will overwinter as C3 or C4-C6 depends in our model on the stage and internal state at the time when the enter-diapause-day (EDD) arrives, a model artifact which may have allowed more compupods to overwinter as C3 than what would naturally occur in this ecosystem. A later descent (EDD) will allow more compupods of the new generation to reach an older stage (C4 +) before descending, and earlier maturation of the population the subsequent spring. Melle and Skjoldal (1998) suggested stage C4 to be the dominant overwintering stage, though at their time of sampling (April–July) this stage is also a major fraction of our model population. In any case, the

mechanism(s) triggering diapause descent remains a central, key question for our understanding of the timing of the population development over a (subsequent) season.

Ice-algae is a central food source for *C. glacialis* early in the season (Søreide et al., 2010). The timing of the initiation of the bloom is central for the food availability and hence development rates for copepods when ascending from diapause in ice-covered regions. Ice-algae production is a complex and poorly understood process (Leu et al., 2015), supposedly first limited by light availability and later by nutrient depletion. Snow cover will also influence ice-algae phenology (Leu et al., 2015). The ice-algae food source in our model is a major simplification of the process knowledge described in Leu et al. (2015). In our model, ice-algae consumption commences in mid-April, in accordance with Søreide et al. (2010). Hegseth (1992) suggests that ice-algae production in the Barents Sea may occur already in March, although ice-algae were not observed in March surveys during the 2018–2021 Nansen Legacy campaigns (A. Wold *pers. comm.*). The magnitude of algae biomass in ice-covered waters is also a large unknown, and *in situ* observations report variation within three orders of magnitude (Tamelander et al., 2009 and references therein). We assumed a maximum level of 100 mg C m^{-2} to be a conservative estimate for this region, which by chance is similar to the biomass of ice-algae in an Ecopath model for the Barents Sea by Pedersen et al. (2021). At this level the growth of *C. glacialis* compupods as parametrized here is limited by food availability when ice algae are the only food source available. The fact that ice-algae and phytoplankton consumption was similar in magnitude was surprising and might be related to that ice-algae are available over a large (ice-covered) area in the model domain and that competition for this food source is not implemented in the model. The timing and magnitude of ice-algae production presumably affects copepod development rates in spring and hence the timing of the seasonal population development. Implementation of a more sophisticated ice-algae module will therefore be a necessary step towards more reliable modelling of *C. glacialis* in the NORWECOM.E2E model system.

4.4. Climate change

The Arctic Ocean is warming considerably faster than the global average, a phenomenon recently termed the "Arctic Ocean Amplification" (Shu et al., 2022). Results from our model are relevant for the discussion of how a changing ocean climate will affect the future distribution of *Calanus* spp. in the Barents Sea. When building this model, we found no mechanistic explanation in the literature for why *C. glacialis* would struggle in more temperate environments. On the contrary, this species seems capable of surviving and reproducing under a broad range of environmental conditions (Choquet et al., 2017, 2018; Daase et al., 2013; Niehoff and Hirche, 2005). As parametrized here, both *C. glacialis* and *C. finmarchicus* would develop faster under increasing temperatures and food availability characteristic of more temperate regions of the model domain. Since lipid content in copepods is related to body size (Record et al., 2018) and growth and development rates for zooplankton are thermally decoupled (Horne et al., 2019), faster development could lead to a smaller-sized and less lipid-rich *Calanus* spp. complex in a warmer Barents Sea (Renaud et al., 2018).

Because it is relatively shallow, advection within the Barents Sea is to a large degree structured by the topography (Ingvaldsen and Loeng, 2009) which will not be altered by a changing climate. Therefore, it seems unlikely that *C. finmarchicus* will become dominant in northern parts of this ecosystem and make a considerable contribution to the resource-competition between grazers in the northern Barents Sea. Water exchange between the Barents Sea and surrounding ocean may, nevertheless, affect the in- and outflow of copepods in this ecosystem, again highlighting the importance of understanding the source of the *C. glacialis* population here. For zooplankton advected into the northern regions, the phenology and quality of primary producers in a warmer climate will likely be key for their survival or lack thereof. Ice algae was an important food source for the modelled population, and loss of sea ice may lead to a mis-match between the timing of copepod food demand and phenology of primary producers (e.g. Søreide et al., 2010). Also, warming is often expected to reduce the size-structure in phytoplankton communities (Finkel et al., 2010; Litchman et al., 2013), which may reduce the availability of suitable resources for large zooplankton like copepods (Hansen et al., 1994).

5. Concluding remarks

While observations give an incomplete access to a natural phenomenon, ecosystem models offer an incomplete representation or parameterization of processes and components of a natural system (Oreskes et al., 1994). In the present study an IBM was built from published knowledge of *C. glacialis* encompassing observed natural variation. In this context the model represents a framework where available information can be integrated and tested to disclose knowledge gaps and possible inconsistencies between independent studies and observational data sets. The use of ecosystem models captures the full advective story of individuals and enables the study of system-wide cause − effect relationships which are impossible purely from observations. Our results suggests that individual variation in development and life cycle length may be a natural result from transportation through environmental gradients supporting the large variation reported from observational studies. Stage C3 may be a more important overwintering stage than previously considered, also supported by monitoring surveys and field campaigns into more Arctic regions of this ecosystem. The model also suggests that the seasonal development and timing of reproduction may be more prolonged when integrating over larger regions in the north. Ocean currents will transport the population over a large area, and there are knowledge-gaps concerning the mechanisms that structures the spatial distribution of this species in Arctic, sub-Arctic and more temperate regions. Temperature alone does not seem to be an appropriate predictor for where *C. glacialis* will thrive or not. With future warming and earlier onset of the spring phytoplankton bloom, we expect faster development of both Arctic and Atlantic *Calanus* species, potentially reducing the life cycle of *C. glacialis* from 2 to 1 years in the northern Barents Sea. The main limitation of the study is the incomplete parameterization of the full *C. glacialis* life cycle, along with the absence of precise information on how to represent complex natural processes which in many cases lack a solid mechanistic understanding. Nevertheless, the use of models and observations together generates synergies and allows both for a better assessment of the system state and an improved ecosystem understanding (Skogen et al., 2021).

Declaration of Competing Interest

The authors declare that they have no known competing financial interests or personal relationships that could have appeared to influence the work reported in this paper.

Data availability

Model data accompanying this article are published at https://doi.org/10.21335/NMDC-1778560190.

Acknowledgements

This work was funded by the Norwegian Research Council through the Nansen Legacy project (RCN project no. 276730). We acknowledge researchers, technicians, and crew from IMR and PINRO who have contributed to collecting and processing the *C. glacialis* data from the Barents Sea monitoring survey in 2013.

Appendix A. Supplementary data

Supplementary data to this article can be found online at https://doi.org/10.1016/j.pocean.2023.103106.

References

Aarflot, J.M., Skjoldal, H.R., Dalpadado, P., Skern-Mauritzen, M., 2018. Contribution of *Calanus* species to the mesozooplankton biomass in the Barents Sea. ICES J. Mar. Sci. 75, 2342–2354. https://doi.org/10.1093/icesjms/fsx221.

Aarflot, J.M., Dalpadado, P., Fiksen, Ø., 2020. Foraging success in planktivorous fish increases with topographic blockage of prey distributions. Mar. Ecol. Prog. Ser. 644, 129–142. https://doi.org/10.3354/meps13343.

Aarflot, J.M., Hjøllo, S.S., Strand, E., Skogen, M.D., 2022. Transportation and predation control structures the distribution of a key calanoid in the Nordic Seas. Prog. Oceanogr. 202, 102761 https://doi.org/10.1016/j.pocean.2022.102761.

Aksnes, D.L., Blindheim, J., 1996. Circulation patterns in the North Atlantic and possible impact on population dynamics of *Calanus finmarchicus*. Ophelia 44, 7–28.

Aksnes, D.L., Ulvestad, K.B., Baliño, B.M., Berntsen, J., Egge, J.K., Svendsen, E., 1995. Ecological modelling in coastal waters: Towards predictive physical-chemical-biological simulation models. Ophelia 41, 5–36. https://doi.org/10.1080/00785236.1995.10422035.

Aksnes, D.L., Utne, A.C.W., 1997. A revised model of visual range in fish. Sarsia 82, 137–147. https://doi.org/10.1080/00364827.1997.10413647.

Arashkevich, E., Wassmann, P., Pasternak, A., Riser, C.W., 2002. Seasonal and spatial changes in biomass, structure, and development progress of the zooplankton community in the Barents Sea. J. Mar. Syst. 38, 125–145.

Bagøien, E., Kaartvedt, S., Aksnes, D.L., Eiane, K., 2001. Vertical distribution and mortality of overwintering *Calanus*. Limnol. Oceanogr. 46, 1494–1510. https://doi.org/10.4319/lo.2001.46.6.1494.

Bailey, A., Thor, P., Browman, H.I., Fields, D.M., Runge, J., Vermont, A., Bjelland, R., Thompson, C., Shema, S., Durif, C.M.F., Hop, H., 2017. Early life stages of the Arctic copepod *Calanus glacialis* are unaffected by increased seawater pCO2. ICES J. Mar. Sci. 74, 996–1004. https://doi.org/10.1093/icesjms/fsw066.

Banas, N.S., Møller, E.F., Nielsen, T.G., Eisner, L.B., 2016. Copepod Life Strategy and Population Viability in Response to Prey Timing and Temperature: Testing a New Model across Latitude, Time, and the Size Spectrum. Front. Mar. Sci. 3 https://doi.org/10.3389/fmars.2016.00225.

Bandara, K., Varpe, Ø., Søreide, J.E., Wallenschus, J., Berge, J., Eiane, K., 2016. Seasonal vertical strategies in a high-Arctic coastal zooplankton community. Mar. Ecol. Prog. Ser. 555, 49–64. https://doi.org/10.3354/meps11831.

Baumgartner, M.F., Tarrant, A.M., 2017. The Physiology and Ecology of Diapause in Marine Copepods. Annu. Rev. Mar. Sci. 9, 387–411. https://doi.org/10.1146/annurev-marine-010816-060505.

Bouchard, C., Fortier, L., 2020. The importance of *Calanus glacialis* for the feeding success of young polar cod: a circumpolar synthesis. Polar Biol. https://doi.org/10.1007/s00300-020-02643-0.

Broms, C., Melle, W., Kaartvedt, S., 2009. Oceanic distribution and life cycle of *Calanus* species in the Norwegian Sea and adjacent waters. Deep Sea Res. Part II Top. Stud. Oceanogr., The Proceedings of the ECONORTH Symposium on Ecosystem Dynamics in the Norwegian Sea and Barents Sea 56, 1910–1921. 10.1016/j.dsr2.2008.11.005.

Campbell, R.G., Ashjian, C.J., Sherr, E.B., Sherr, B.F., Lomas, M.W., Ross, C., Alatalo, P., Gelfman, C., Keuren, D.V., 2016. Mesozooplankton grazing during spring sea-ice conditions in the eastern Bering Sea. Deep Sea Res. Part II Top. Stud. Oceanogr. Understand. Ecosyst. Process. Eastern Bering Sea IV 134, 157–172. https://doi.org/10.1016/j.dsr2.2015.11.003.

Campbell, R.G., Sherr, E.B., Ashjian, C.J., Plourde, S., Sherr, B.F., Hill, V., Stockwell, D. A., 2009. Mesozooplankton prey preference and grazing impact in the western Arctic Ocean. Deep Sea Res. Part II Top. Stud. Oceanogr., The Western Artic Shelf-Basin Interactions (SBI)Project, Vol.2 56, 1274–1289. 10.1016/j.dsr2.2008.10.027.

Carlotti, F., Wolf, K.-U., 1998. A Lagrangian ensemble model of *Calanus finmarchicus* coupled with a 1D ecosystem model. Fish. Oceanogr. 7 (191–204), x.

Carmack, E., Barber, D., Christensen, J., Macdonald, R., Rudels, B., Sakshaug, E., 2006. Climate variability and physical forcing of the food webs and the carbon budget on panarctic shelves. Prog. Oceanogr., Structure and function of contemporary food webs on Arctic shelves: a pan-Arctic comparison 71, 145–181. 10.1016/j.pocean.2006.10.005.

Choquet, M., Hatlebakk, M., Dhanasiri, A.K.S., Kosobokova, K., Smolina, I., Søreide, J.E., Svensen, C., Melle, W., Kwaśniewski, S., Eiane, K., Daase, M., Tverberg, V., Skreslet, S., Bucklin, A., Hoarau, G., 2017. Genetics redraws pelagic biogeography of *Calanus*. Biol. Lett. 13 (20170588), 2017.

Cleary, A.C., Søreide, J.E., Freese, D., Niehoff, B., Gabrielsen, T.M., Handling editor: David Fields, 2017. Feeding by *Calanus glacialis* in a high arctic fjord: potential seasonal importance of alternative prey. ICES J. Mar. Sci. 74, 1937–1946. 10.1093/icesjms/fsx106.

Comiso, J.C., Hall, D.K., 2014. Climate trends in the Arctic as observed from space. WIREs Clim. Change 5, 389–409. https://doi.org/10.1002/wcc.277.

Corkett, C.J., McLaren, I.A., Sevigny, J.M., 1986. The rearing of the marine calanoid copepods *Calanus finmarchicus* (Gunnerus), *C. glacialis* Jaschnov and *C. hyperboreus* Krøyer with comments on the equiproportional rule. Syllogeus 58, 539–546.

Daase, M., Eiane, K., Aksnes, D.L., Vogedes, D., 2008. Vertical distribution of *Calanus* spp. and *Metridia longa* at four Arctic locations. Mar. Biol. Res. 4, 193–207. https://doi.org/10.1080/17451000801907948.

Daase, M., Falk-Petersen, S., Varpe, Ø., Darnis, G., Søreide, J.E., Wold, A., Leu, E., Berge, J., Philippe, B., Fortier, L., 2013. Timing of reproductive events in the marine copepod *Calanus glacialis*: a pan-Arctic perspective. Can. J. Fish. Aquat. Sci. 70, 871–884. https://doi.org/10.1139/cjfas-2012-0401.

Daase, M., Kosobokova, K., Last, K., Cohen, J., Choquet, M., Hatlebakk, M., Søreide, J., 2018. New insights into the biology of *Calanus* spp. (Copepoda) males in the Arctic. Mar. Ecol. Prog. Ser. 607, 53–69. https://doi.org/10.3354/meps12788.

Daase, M., Søreide, J.E., 2021. Seasonal variability in non-consumptive mortality of Arctic zooplankton. J. Plankton Res. 43, 565–585. https://doi.org/10.1093/plankt/fbab042.

Daase, M., Søreide, J.E., Martynova, D., 2011. Effects of food quality on naupliar development in *Calanus glacialis* at subzero temperatures. Mar. Ecol. Prog. Ser. 429, 111–124. https://doi.org/10.3354/meps09075.

Dalpadado, P., Arrigo, K.R., van Dijken, G.L., Rune Skjoldal, H., Bagøien, E., Dolgov, A., Prokopchuk, I., Sperfeld, E., 2020. Climate effects on temporal and spatial dynamics of phytoplankton and zooplankton in the Barents Sea. Prog. Oceanogr. 102320 https://doi.org/10.1016/j.pocean.2020.102320.

DeAngelis, D.L., Grimm, V., 2014. Individual-based models in ecology after four decades. F1000Prime Rep. 6, 39. https://doi.org/10.12703/P6-39.

Eriksen, E., Skjoldal, H.R., Gjøsæter, H., Primicerio, R., 2017. Spatial and temporal changes in the Barents Sea pelagic compartment during the recent warming. Prog. Oceanogr. 151, 206–226. https://doi.org/10.1016/j.pocean.2016.12.009.

Eriksen, E., Huserbråten, M., Gjøsæter, H., Vikebø, F., Albretsen, J., 2019. Polar cod egg and larval drift patterns in the Svalbard archipelago. Polar Biol. https://doi.org/10.1007/s00300-019-02549-6.

Ershova, E.A., Kosobokova, K.N., Banas, N.S., Ellingsen, I., Niehoff, B., Hildebrandt, N., Hirche, H.-J., 2021. Sea ice decline drives biogeographical shifts of key *Calanus* species in the central Arctic Ocean. Glob. Change Biol. 27, 2128–2143. https://doi.org/10.1111/gcb.15562.

Falk-Petersen, S., Hop, H., Budgell, W.P., Hegseth, E.N., Korsnes, R., Løyning, T.B., Børre Ørbæk, J., Kawamura, T., Shirasawa, K., 2000b. Physical and ecological processes in the marginal ice zone of the northern Barents Sea during the summer melt period. J. Mar. Syst., Hydrodynamical and Ecosystem Processes in Ice-covered Seas of the 27, 131–159. 10.1016/S0924-7963(00)00064-6.

Falk-Petersen, S., Hagen, W., Kattner, G., Clarke, A., Sargent, J., 2000a. Lipids, trophic relationships, and biodiversity in Arctic and Antarctic krill. Can. J. Fish. Aquat. Sci. 57, 178–191. https://doi.org/10.1139/f00-194.

Falk-Petersen, S., Dahl, T.M., Scott, C.L., Sargent, J.R., Gulliksen, B., Kwasniewski, S., Hop, H., Millar, R.-M., 2002. Lipid biomarkers and trophic linkages between ctenophores and copepods in Svalbard waters. Mar. Ecol. Prog. Ser. 227, 187–194. https://doi.org/10.3354/meps227187.

Falk-Petersen, S., Mayzaud, P., Kattner, G., Sargent, J., 2009. Lipids and life strategy of Arctic *Calanus*. Mar. Biol. Res. 5, 18–39. https://doi.org/10.1080/17451000802512267.

Fiksen, Ø., 2000. The adaptive timing of diapause – a search for evolutionarily robust strategies in Calanus finmarchicus. ICES J. Mar. Sci. 57, 1825–1833. https://doi.org/10.1006/jmsc.2000.0976.

Fiksen, Ø., Carlotti, F., 1998. A model of optimal life history and diel vertical migration in *Calanus finmarchicus*. Sarsia.

Finkel, Z.V., Beardall, J., Flynn, K.J., Quigg, A., Rees, T.A.V., Raven, J.A., 2010. Phytoplankton in a changing world: cell size and elemental stoichiometry. J. Plankton Res. 32, 119–137. https://doi.org/10.1093/plankt/fbp098.

Freese, D., Søreide, J.E., Graeve, M., Niehoff, B., 2016. A year-round study on metabolic enzymes and body composition of the Arctic copepod *Calanus glacialis*: implications for the timing and intensity of diapause. Mar. Biol. 164, 3. https://doi.org/10.1007/s00227-016-3036-2.

Grimm, V., Berger, U., Bastiansen, F., Eliassen, S., Ginot, V., Giske, J., Goss-Custard, J., Grand, T., Heinz, S.K., Huse, G., Huth, A., Jepsen, J.U., Jørgensen, C., Mooij, W.M., Müller, B., Pe'er, G., Piou, C., Railsback, S.F., Robbins, A.M., Robbins, M.M., Rossmanith, E., Rüger, N., Strand, E., Souissi, S., Stillman, R.A., Vabø, R., Visser, U., DeAngelis, D.L., 2006. A standard protocol for describing individual-based and agent-based models. Ecol. Model. 198, 115–126. https://doi.org/10.1016/j.ecolmodel.2006.04.023.

Grimm, V., Berger, U., DeAngelis, D.L., Polhill, J.G., Giske, J., Railsback, S.F., 2010. The ODD protocol: A review and first update. Ecol. Model. 221, 2760–2768. https://doi.org/10.1016/j.ecolmodel.2010.08.019.

Grimm, V., Railsback, S.F., Vincenot, C.E., Berger, U., Gallagher, C., DeAngelis, D.L., Edmonds, B., Ge, J., Giske, J., Groeneveld, J., Johnston, A.S.A., Milles, A., Nabe-Nielsen, J., Polhill, J.G., Radchuk, V., Rohwäder, M.-S., Stillman, R.A., Thiele, J.C., Ayllón, D., 2020. The ODD Protocol for Describing Agent-Based and Other Simulation Models: A Second Update to Improve Clarity, Replication, and Structural Realism. J. Artif. Soc. Soc. Simul. 23, 7. https://doi.org/10.18564/jasss.4259.

Grote, U., Pasternak, A., Arashkevich, E., Halvorsen, E., Nikishina, A., 2015. Thermal response of ingestion and egestion rates in the Arctic copepod *Calanus glacialis* and possible metabolic consequences in a warming ocean. Polar Biol. 38, 1025–1033. https://doi.org/10.1007/s00300-015-1664-5.

Hansen, B., Bjornsen, P.K., Hansen, P.J., 1994. The size ratio between planktonic predators and their prey. Limnol. Oceanogr. 39, 395–403. https://doi.org/10.4319/lo.1994.39.2.0395.

Hansen, C., Skogen, M.D., Utne, K.R., Broms, C., Strand, E., Hjøllo, S.S., 2021. Patterns, efficiency and ecosystem effects when fishing *Calanus finmarchicus* in the Norwegian Sea using an individual-based model. Mar. Ecol. Prog. Ser. 680, 15–32. https://doi.org/10.3354/meps13942.

Hegseth, E.N., 1992. Sub-ice algal assemblages of the Barents Sea: Species composition, chemical composition, and growth rates. Polar Biol. 12, 485–496. https://doi.org/10.1007/BF00238187.

Hirche, H.-J., 1989. Egg production of the Arctic copepod *Calanus glacialis*: laboratory experiments. Mar. Biol. 103, 311–318. https://doi.org/10.1007/BF00397264.
Hirche, H., Bohrer, R.N., 1987. Reproduction of the Arctic copepod *Calanus glacialis* in Fram Strait. Mar. Biol. 94, 11–17. https://doi.org/10.1007/BF00392894.
Hirche, H., Kosobokova, K., 2003. Early reproduction and development of dominant calanoid copepods in the sea ice zone of the Barents Sea—need for a change of paradigms? Mar. Biol. 143, 769–781. https://doi.org/10.1007/s00227-003-1122-8.
Hirche, H.-J., Kosobokova, K., 2007. Distribution of *Calanus finmarchicus* in the northern North Atlantic and Arctic Ocean—Expatriation and potential colonization. Deep Sea Res. Part II Top. Stud. Oceanogr. 54, 2729–2747. https://doi.org/10.1016/j.dsr2.2007.08.006.
Hirche, H., Kwasniewski, S., 1997. Distribution, reproduction and development of *Calanus* species in the Northeast Water in relation to environmental conditions. J. Mar. Syst. 10, 299–317. https://doi.org/10.1016/s0924-7963(96)00057-7.
Hjøllo, S., Hansen, C., Skogen, M., 2021. Assessing the importance of zooplankton sampling patterns with an ecosystem model. Mar. Ecol. Prog. Ser. DYNMODav1 https://doi.org/10.3354/meps13774.
Hjøllo, S.S., Huse, G., Skogen, M.D., Melle, W., 2012. Modelling secondary production in the Norwegian Sea with a fully coupled physical/primary production/individual-based *Calanus finmarchicus* model system. Mar. Biol. Res. 8, 508–526. https://doi.org/10.1080/17451000.2011.642805.
Hobbs, L., Banas, N.S., Cottier, F.R., Berge, J., Daase, M., 2020. Eat or Sleep: Availability of Winter Prey Explains Mid-Winter and Spring Activity in an Arctic *Calanus* Population. Front. Mar. Sci. 7, 744. https://doi.org/10.3389/fmars.2020.541564.
Horne, C.R., Hirst, A.G., Atkinson, D., Almeda, R., Kiørboe, T., 2019. Rapid shifts in the thermal sensitivity of growth but not development rate causes temperature–size response variability during ontogeny in arthropods. Oikos 128, 823–835. https://doi.org/10.1111/oik.06016.
Huse, G., Melle, W., Skogen, M.D., Hjøllo, S.S., Svendsen, E., Budgell, W.P., 2018. Modeling Emergent Life Histories of Copepods. Front. Ecol. Evol. 6 https://doi.org/10.3389/fevo.2018.00023.
Huse, G., Toresen, R., 1996. A comparative study of the feeding habits of herring (*Clupea harengus*, clupeidae, L.) and capelin (*Mallotus villosus*, osmeridae, Müller) in the Barents Sea. Sarsia 81, 143–153. https://doi.org/10.1080/00364827.1996.10413618.
Huserbråten, M.B.O., Eriksen, E., Gjøsæter, H., Vikebø, F., 2019. Polar cod in jeopardy under the retreating Arctic sea ice. Commun. Biol. 2, 1–8. https://doi.org/10.1038/s42003-019-0649-2.
ICES, 2021. Working Group on the Integrated Assessments of the Barents Sea (WGIBAR). ICES Sci. Rep. 3 https://doi.org/10.17895/ices.pub.8241.
ICES, 2018. Report of the Arctic Fisheries Working Group, Ispra, Italy, 16-24 April 2018. (No. ICES C.M. 2018/ACOM:06). Italy.
Ingvaldsen, R.B., Assmann, K.M., Primicerio, R., Fossheim, M., Polyakov, I.V., Dolgov, A. V., 2021. Physical manifestations and ecological implications of Arctic Atlantification. Nat. Rev. Earth Environ. 1–16 https://doi.org/10.1038/s43017-021-00228-x.
Ingvaldsen, R., Loeng, H., 2009. Physical oceanography. In: Sakshaug, E., Johnsen, G., Kovacs, K.M. (Eds.), Ecosystem Barents Sea. Tapir Academic Press, Trondheim, pp. 33–64.
Jaschnov, W.A., 1970. Distribution of <i>Calanus<i> species in the seas of the Northern Hemisphere. Int. Rev. Gesamten Hydrobiol. Hydrogr. 55, 197–212.
Ji, R., Ashjian, C.J., Campbell, R.G., Chen, C., Gao, G., Davis, C.S., Cowles, G.W., Beardsley, R.C., 2012. Life history and biogeography of *Calanus* copepods in the Arctic Ocean: An individual-based modeling study. Prog. Oceanogr. 96, 40–56. https://doi.org/10.1016/j.pocean.2011.10.001.
Jung-Madsen, S., Nielsen, T.G., 2015. Early development of *Calanus glacialis* and *C. finmarchicus*. Limnol. Oceanogr. 60, 934–946. https://doi.org/10.1002/lno.10070.
Juul-Pedersen, T., Nielsen, T.G., Michel, C., Møller, E.F., Tiselius, P., Thor, P., Olesen, M., Selander, E., Gooding, S., 2006. Sedimentation following the spring bloom in Disko Bay, West Greenland, with special emphasis on the role of copepods. Mar. Ecol. Prog. Ser. 314, 239–255. https://doi.org/10.3354/meps314239.
Karnovsky, N., Kwasniewski, S., Weslawski, J., Walkusz, W., Beszczynska-Möller, A., 2003. Foraging behavior of little auks in a heterogeneous environment. Mar. Ecol. Prog. Ser. 253, 289–303. https://doi.org/10.3354/meps253289.
Kattner, G., Hagen, W., 2009. Lipids in marine copepods: latitudinal characteristics and perspective to global warming. In: Kainz, M., Brett, M.T., Arts, M.T. (Eds.), Lipids in Aquatic Ecosystems. Springer, New York, New York, NY, pp. 257–280. https://doi.org/10.1007/978-0-387-89366-2_11.
Langbehn, T.J., Aarflot, J.M., Freer, J.J., Varpe, Ø., 2023. Visual predation risk and spatial distributions of large Arctic copepods along gradients of sea ice and bottom depth. Limnol. Oceanogr. 68, 1388–1405. https://doi.org/10.1002/lno.12354.
Lee, R.F., Hagen, W., Kattner, G., 2006. Lipid storage in marine zooplankton. Mar. Ecol. Prog. Ser. 307, 273–306. https://doi.org/10.3354/meps307273.
Leu, E., Mundy, C.J., Assmy, P., Campbell, K., Gabrielsen, T.M., Gosselin, M., Juul-Pedersen, T., Gradinger, R., 2015. Arctic spring awakening – Steering principles behind the phenology of vernal ice algal blooms. Prog. Oceanogr. Overarching perspectives of contemporary and future ecosystems in the Arctic Ocean 139, 151–170. https://doi.org/10.1016/j.pocean.2015.07.012.
Lien, V., Gusdal, Y., Albretsen, J., Melsom, F., Vikebø, F., 2013. Evaluation of a Nordic Seas 4 km numerical ocean model hindcast archive (SVIM), 1960-2011. Fisk. Og Havet 7.
Lind, S., Ingvaldsen, R.B., Furevik, T., 2018. Arctic warming hotspot in the northern Barents Sea linked to declining sea-ice import. Nat. Clim. Change 8, 634. https://doi.org/10.1038/s41558-018-0205-y.
Litchman, E., Ohman, M.D., Kiørboe, T., 2013. Trait-based approaches to zooplankton communities. J. Plankton Res. 35, 473–484. https://doi.org/10.1093/plankt/fbt019.
Loeng, H., 1991. Features of the physical oceanographic conditions of the Barents Sea. Polar Res. 10, 5–18. https://doi.org/10.1111/j.1751-8369.1991.tb00630.x.
Madsen, S.D., Nielsen, T.G., Hansen, B.W., 2001. Annual population development and production by *Calanus finmarchicus*, *C. glacialis* and *C. hyperboreus* in Disko Bay, western Greenland. Mar. Biol. 139, 75–93.
Madsen, S.J., Nielsen, T.G., Tervo, O.M., Soderkvist, J., 2008. Importance of feeding for egg production in *Calanus finmarchicus* and *C. glacialis* during the Arctic spring. Mar. Ecol. Prog. Ser. 353, 177–190. https://doi.org/10.3354/meps07129.
Maps, F., Record, N.R., Pershing, A.J., 2014. A metabolic approach to dormancy in pelagic copepods helps explaining inter- and intra-specific variability in life-history strategies. J. Plankton Res. 36, 18–30. https://doi.org/10.1093/plankt/fbt100.
Melle, W., Skjoldal, H.R., 1998. Reproduction and development of *Calanus finmarchicus*, *C. glacialis* and *C. hyperboreus* in the Barents Sea. Mar. Ecol. Prog. Ser. 169, 211–228. https://doi.org/10.3354/meps169211.
Niehoff, B., Hirche, H.-J., 2005. Reproduction of *Calanus glacialis* in the Lurefjord (western Norway): indication for temperature-induced female dormancy. Mar. Ecol. Prog. Ser. 285, 107–115. https://doi.org/10.3354/meps285107.
Norwegian Meteorological Institute, Institute Of Marine Research, 2015. SVIM ocean hindcast archive. Norstore. 10.11582/2015.00014.
Ohman, M.D., Romagnan, J.-B., 2016. Nonlinear effects of body size and optical attenuation on Diel Vertical Migration by zooplankton. Limnol. Oceanogr. 61, 765–770. https://doi.org/10.1002/lno.10251.
Onarheim, I.H., Eldevik, T., Smedsrud, L.H., Stroeve, J.C., 2018. Seasonal and Regional Manifestation of Arctic Sea Ice Loss. J. Clim. 31, 4917–4932. https://doi.org/10.1175/JCLI-D-17-0427.1.
Oreskes, N., Shrader-Frechette, K., Belitz, K., 1994. Verification, Validation, and Confirmation of Numerical Models in the Earth Sciences. Science 263, 641–646. https://doi.org/10.1126/science.263.5147.641.
Orlova, E., Dalpadado, P., Knutsen, T., Nesterova, V.N., Prokopchuk, I.P., 2011. Zooplankton. In: Jakobsen, T., Ožigin, V.K. (Eds.), The Barents Sea : Ecosystem, Resources, Management : Half a Century of Russian-Norwegian Cooperation. Tapir Academic Press, Trondheim, pp. 91–119.
Orlova, E.L., Dolgov, A.V., Rudneva, G.B., Oganin, I.A., Konstantinova, L.L., 2009. Trophic relations of capelin *Mallotus villosus* and polar cod *Boreogadus saida* in the Barents Sea as a factor of impact on the ecosystem. Deep-Sea Res. Part Ii-Top. Stud. Oceanogr. 56, 2054–2067. https://doi.org/10.1016/j.dsr2.2008.11.016.
Pasternak, A., Wexels Riser, C., Arashkevich, E., Rat'kova, T., Wassmann, P., 2002. *Calanus* spp. grazing affects egg production and vertical carbon flux (the marginal ice zone and open Barents Sea). J. Mar. Syst., Seasonal C-cycling variability in the open and ice-covered waters of the Barents Sea 38, 147–164. 10.1016/S0924-7963(02)00174-4.
Pedersen, T., Mikkelsen, N., Lindstrøm, U., Renaud, P.E., Nascimento, M.C., Blanchet, M.-A., Ellingsen, I.H., Jørgensen, L.L., Blanchet, H., 2021. Overexploitation, Recovery, and Warming of the Barents Sea Ecosystem During 1950–2013. Front. Mar. Sci. 8, 1291. https://doi.org/10.3389/fmars.2021.732637.
Record, N.R., Ji, R., Maps, F., Varpe, Ø., Runge, J.A., Petrik, C.M., Johns, D., 2018. Copepod diapause and the biogeography of the marine lipidscape. J. Biogeogr. https://doi.org/10.1111/jbi.13414.
Renaud, P.E., Daase, M., Banas, N.S., Gabrielsen, T.M., Søreide, J.E., Varpe, Ø., Cottier, F., Falk-Petersen, S., Halsband, C., Vogedes, D., Heggland, K., Berge, J., 2018. Pelagic food-webs in a changing Arctic: a trait-based perspective suggests a mode of resilience. ICES J. Mar. Sci. 75, 1871–1881. https://doi.org/10.1093/icesjms/fsy063.
Runge, J.A., Ingram, R.G., 1991. Under-ice feeding and diel migration by the planktonic copepods *Calanus glacialis* and *Pseudocalanus minutus* in relation to the ice algal production cycle in southeastern Hudson Bay. Canada. Mar. Biol. 108, 217–225. https://doi.org/10.1007/BF01344336.
Scheffer, M., Baveco, J.M., DeAngelis, D.L., Rose, K.A., van Nes, E.H., 1995. Super-individuals a simple solution for modelling large populations on an individual basis. Ecol. Model. 80, 161–170. https://doi.org/10.1016/0304-3800(94)00055-M.
Scott, C.L., Falk-Petersen, S., Gulliksen, B., Lønne, O.-J., Sargent, J.R., 2001. Lipid indicators of the diet of the sympagic amphipod *Gammarus wilkitzkii* in the Marginal Ice Zone and in open waters of Svalbard (Arctic). Polar Biol. 24, 572–576. https://doi.org/10.1007/s003000100252.
Shchepetkin, A.F., McWilliams, J.C., 2005. The regional oceanic modeling system (ROMS): a split-explicit, free-surface, topography-following-coordinate oceanic model. Ocean Model. 9, 347–404. https://doi.org/10.1016/j.ocemod.2004.08.002.
Shu, Q., Wang, Q., Årthun, M., Wang, S., Song, Z., Zhang, M., Qiao, F., 2022. Arctic Ocean Amplification in a warming climate in CMIP6 models. Sci. Adv. 8, eabn9755. https://doi.org/10.1126/sciadv.abn9755.
Skjoldal, H.R., Gjøsæter, H., Loeng, H., 1992. The Barents Sea ecosystem in the 1980s: ocean climate, plankton, and capelin growth. ICES Mar. Sci. Symp. 195, 278–290.
Skogen, M.D., Svendsen, E., Berntsen, J., Aksnes, D., Ulvestad, K.B., 1995. Modelling the primary production in the North Sea using a coupled three-dimensional physical-chemical-biological ocean model. Estuar. Coast. Shelf Sci. 41, 545–565. https://doi.org/10.1016/0272-7714(95)90026-8.
Skogen, M.D., Budgell, W.P., Rey, F., 2007. Interannual variability in Nordic seas primary production. ICES J. Mar. Sci. 64, 889–898. https://doi.org/10.1093/icesjms/fsm063.
Skogen, M.D., Ji, R., Akimova, A., Daewel, U., Hansen, C., Hjøllo, S.S., van Leeuwen, S. M., Maar, M., Macias, D., Mousing, E.A., Almroth-Rosell, E., Sailley, S.F., Spence, M. A., Troost, T.A., van de Wolfshaar, K., 2021. In: Disclosing the truth: Are models better than observations?. https://doi.org/10.3354/meps13574.

Slagstad, D., Tande, K.S., 1990. Growth and production dynamics of *Calanus glacialis* in an arctic pelagic food web. Mar. Ecol. Prog. Ser. 63, 189–199. https://doi.org/10.3354/meps063189.

Søiland, H., Huse, G., 2012. Using RAFOS floats to simulate overwinter transport of *Calanus finmarchicus* in the Norwegian Sea. Mar. Biol. Res. 8, 502–507. https://doi.org/10.1080/17451000.2011.639780.

Søreide, J.E., Falk-Petersen, S., Hegseth, E.N., Hop, H., Carroll, M.L., Hobson, K.A., Blachowiak-Samolyk, K., 2008. Seasonal feeding strategies of *Calanus* in the high-Arctic Svalbard region. Deep-Sea Res. Part Ii-Top. Stud. Oceanogr. 55, 2225–2244. https://doi.org/10.1016/j.dsr2.2008.05.024.

Søreide, J.E., Leu, E., Berge, J., Graeve, M., Falk-Petersen, S., 2010. Timing of blooms, algal food quality and *Calanus glacialis* reproduction and growth in a changing Arctic. Glob. Change Biol. 16, 3154–3163. https://doi.org/10.1111/j.1365-2486.2010.02175.x.

Steen, H., Vogedes, D., Broms, F., Falk-Petersen, S., Berge, J., 2007. Little auks (*Alle alle*) breeding in a High Arctic fjord system: bimodal foraging strategies as a response to poor food quality? Polar Res. 26, 118–125. https://doi.org/10.1111/j.1751-8369.2007.00022.x.

Stige, L.C., Dalpadado, P., Orlova, E., Boulay, A.-C., Durant, J.M., Ottersen, G., Stenseth, N.C., 2014. Spatiotemporal statistical analyses reveal predator-driven zooplankton fluctuations in the Barents Sea. Prog. Oceanogr. 120, 243–253. https://doi.org/10.1016/j.pocean.2013.09.006.

Strand, E., Bagøien, E., Edwards, M., Broms, C., Klevjer, T., 2020. Spatial distributions and seasonality of four *Calanus* species in the Northeast Atlantic. Prog. Oceanogr. 185, 102344 https://doi.org/10.1016/j.pocean.2020.102344.

Svensen, C., Halvorsen, E., Vernet, M., Franzè, G., Dmoch, K., Lavrentyev, P.J., Kwasniewski, S., 2019. Zooplankton Communities Associated With New and Regenerated Primary Production in the Atlantic Inflow North of Svalbard. Front. Mar. Sci. 6.

Tamelander, T., Reigstad, M., Hop, H., Ratkova, T., 2009. Ice algal assemblages and vertical export of organic matter from sea ice in the Barents Sea and Nansen Basin (Arctic Ocean). Polar Biol. 32, 1261. https://doi.org/10.1007/s00300-009-0622-5.

Tande, K.S., 1991. *Calanus* in the North Norwegian fjords and in the Barents Sea. Polar Res. 10, 389–407. https://doi.org/10.1111/j.1751-8369.1991.tb00661.x.

Tande, K., Hassel, A., Slagstad, D., 1985. Gonad maturation and possible life cycle strategies in *Calanus finmarchicus* and *Calanus glacialis* in the northwestern part of the Barents Sea. In: Gray, J.S., Christiansen, M.E. (Eds.), Marine Biology of Polar Regions and Effects of Stress on Marine Organisms. Wiley and Sons, New York, pp. 141–155.

Utne, K.R., Hjøllo, S.S., Huse, G., Skogen, M., 2012. Estimating the consumption of *Calanus finmarchicus* by planktivorous fish in the Norwegian Sea using a fully coupled 3D model system. Mar. Biol. Res. 8, 527–547. https://doi.org/10.1080/17451000.2011.642804.

Varpe, Ø., Jørgensen, C., Tarling, G.A., Fiksen, Ø., 2009. The adaptive value of energy storage and capital breeding in seasonal environments. Oikos 118, 363–370. https://doi.org/10.1111/j.1600-0706.2008.17036.x.

Varpe, Ø., Daase, M., Kristiansen, T., 2015. A fish-eye view on the new Arctic lightscape. ICES J. Mar. Sci. 72, 2532–2538. https://doi.org/10.1093/icesjms/fsv129.

Visser, A.W., Grønning, J., Jónasdóttir, S.H., 2017. *Calanus hyperboreus* and the lipid pump. Limnol. Oceanogr. 62, 1155–1165. https://doi.org/10.1002/lno.10492.

Vogedes, D., Eiane, K., Båtnes, A.S., Berge, J., 2014. Variability in *Calanus* spp. abundance on fine- to mesoscales in an Arctic fjord: implications for little auk feeding. Mar. Biol. Res. 10, 437–448. https://doi.org/10.1080/17451000.2013.815781.

Weydmann, A., Coelho, N.C., Serrão, E.A., Burzyński, A., Pearson, G.A., 2016. Pan-Arctic population of the keystone copepod *Calanus glacialis*. Polar Biol. 39, 2311–2318. https://doi.org/10.1007/s00300-016-1898-x.

Wold, A., Darnis, G., Søreide, J.E., Leu, E., Philippe, B., Fortier, L., Poulin, M., Kattner, G., Graeve, M., Falk-Petersen, S., 2011. Life strategy and diet of *Calanus glacialis* during the winter–spring transition in Amundsen Gulf, south-eastern Beaufort Sea. Polar Biol. 34, 1929–1946. https://doi.org/10.1007/s00300-011-1062-6.